Research Square

Preprints are preliminary reports that have not undergone peer review.
They should not be considered conclusive, used to inform clinical practice,
or referenced by the media as validated information.

Synergistic Thermo-Hydrodynamic Enhancement in Ternary Hybrid Nanofluids (THN) Stabilized in Ethylene Glycol– Distilled Water Mixture (EG@DW 50:50)

Waqar Ahmed

waqarum.ah@gmail.com

Fudan University

Shahid Mehmood

Mohammed V University

S.N Kazi

University of Malaya

Zhan Yiqiang

Fudan University

Research Article

Keywords: Nanofluids, Ternay Hybrid Materials, Heat Transfer, Stability, Thermal Properties

Posted Date: October 29th, 2026

DOI: https://doi.org/10.21203/rs.3.rs-10948655/v1

License: This work is licensed under a Creative Commons Attribution 4.0 International License.
Read Full License

Additional Declarations: No competing interests reported.

Synergistic Thermo-Hydrodynamic Enhancement in Ternary Hybrid Nanofluids (THN) Stabilized in Ethylene Glycol–Distilled Water Mixture (EG@DW 50:50)

Waqar Ahmed[1*], Shahid Mehmood[2], S.N Kazi[3], Yiqiang Zhan[1*]

[1] The State Key Laboratory of Photovoltaic Science and Technology, College of Future Information Technology, Fudan University, Shanghai 200438, China

[2] College of Chemical Sciences and Engineering (CCSE), Laboratory of Inorganic Materials for Sustainable Energy Technologies (LIMSET), University Mohammed VI Polytechnic (UM6P), Benguerir, 43150, Morocco

[3] Faculty of Engineering, Department of Mechanical Engineering, University of Malaya

Corresponding Authors:

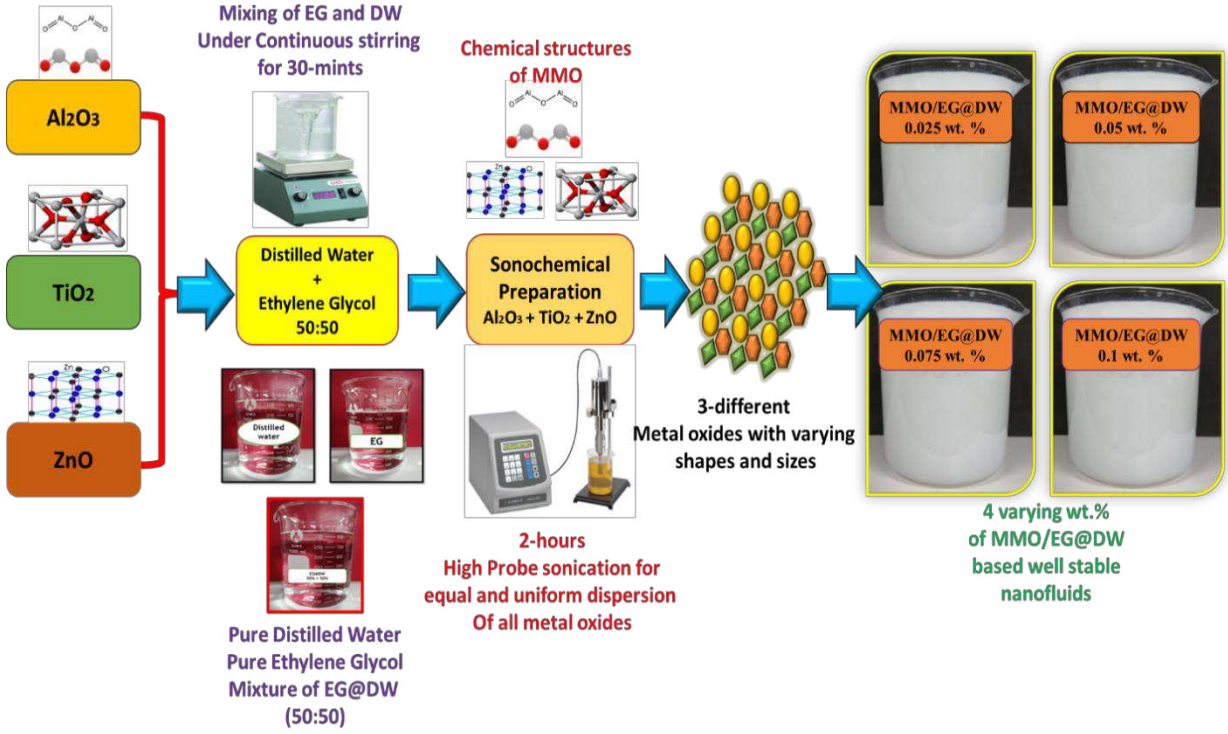
1. **Waqar Ahmed**

waqarum.ah@gmail.com

2. **Yiqiang Zhan**

yqzhan@fudan.edu.cn

GRAPHICAL ABSTRACT



HIGHLIGHTS

- An approach to prepare metal oxide based ternary hybrid nanofluid via a sonochemical process.
- Well dispersed and stable ternary hybrid nanofluids were synthesized using three metal oxides.
- Significant changes in thermophysical characteristics were observed using ternary metal oxides.
- Positive enhancement was recorded in the heat transfer coefficient using ternary metal oxides together.
- Prominent hydrodynamic characteristics were achieved, which are important for enhanced performance.

ABSTRACT

The synthesis of homogeneous and well dispersed mixed metal oxide (MMO) in a mixture of Ethylene Glycol and Distilled Water (EG@DW, 50:50) mixture is established using 2-Step probe sonication, ZnO, Al_2O_3, and TiO2 as an MMO/EG@DW based ternary hybrid nanofluids (THN) were prepared to evaluate the thermophysical, hydrodynamic and convective heat transfer coefficient (CHTC) characteristics in a closed straight stainless steel based circular geometry heat exchanger subjected to a constant heat flux of 10092.41 W m-2. All the metal oxides with different sizes and morphologies were taken at an equal 33.3 % weight and dispersed in EG@DW base fluid at four varying concentrations: 0.025 wt.%, 0.05 wt.%, 0.075 wt.% and 0.1 wt.% to attain well-dispersed hybrid nanofluids. The FESEM, UV-vis, and wt.% absorbance characterizations were carried out to see the uniform dispersion of all particles. The dynamic/kinematic viscosities, density, and thermal conductivity were evaluated at varying temperatures from 20ºC to 45ºC and varying wt.% concentrations. A significant improvement in all parameters was noticed when all metal oxides were loaded together in the EG@DW base fluid. The photograph sedimentation test was employed to assess the longer-term stability and suspension of all particles, and the results revealed surprising stability up to 7 weeks after preparation. Following the confirmation of the experimental analytical correlation, different test runs for MMO/EG@DW-based THN were conducted through a circular geometry heat exchanger in turbulent regions. A prominent enhancement in CHTC and Nusselt numbers was recorded on average and locally against varying Reynolds (Re) numbers from 5849 to 24544. The 0.1 wt.% concentration contributed a higher enhancement of 3120 W m−2 K−1 in CHTC of the MMO/EG@DW based THN with a slight increase in applied pumping power, which is due to the use of EG with DW. Further, the study stated that all the positive parameters at all Reynolds ranges and wt.% concentrations of

MMO/EG@DW based THN offered the possible use of mixed metal oxides hybrid/composite aqueous suspension, together as an alternative working liquid in varying thermal management systems.

Keywords: Nanofluids; Ternay Hybrid Materials; Heat Transfer; Stability; Thermal Properties

Nomenclatures:			
CHTC	Convective Heat Transfer Coefficient	***MMO***	Mixed metal oxides
THN	Ternary hybrid nanofluids	***EG***	Ethylene Glycol
DW	Distilled water	***Q***	Heat flux, *W2.K-1*
A	Surface area (Heat Exchanger), *m2*	***V***	Voltage, *V*
D	Diameter (Heat Exchanger), *m*	***T***	Temperature, *ºC*
FESEM	Field Scanning Electron Microscopy	***I***	Current, *A*
L	Length (Heat Exchanger), *m*	***v***	Velocity, *m.s-1*
Pr	Prandtl numbers	T_w	Wall temperature, *ºC*
Nu	Nusselt Numbers	T_b	Bulk temperature, *ºC*
Re	Reynold Numbers	T_{outlet}	Outlet temperature, *ºC*
T_{inlet}	Inlet temperature, *ºC*	***h***	Heat transfer, *W/m-1.K-1*
f	Friction factor	***wt.%***	Concentrations
k	Thermal conductivity, *W.m-1K-1*		
Subscripts:		**Greek Symbols:**	
b_f	Base Fluid/Liquid	μ	Dynamic viscosity, mPa.s
n_f	Nanofluid	ρ	Fluid/Nanofluid density, kg m-3
b	Bulk	Δp	Pressure drop, Pa

1. INTRODUCTION

Over several years, nanofluids have been capable of heat transfer and have been widely used in a variety of applications like engine cooling, microchannel cooling, nuclear reactors, spacecraft, electronic cooling, tower cooling, transformer cooling, and many more thermal systems. Due to the rising demand for lubricants in engineering industries, the potential use of nanofluids is becoming a trending research topic in both industry and academia [1]. Similarly, advances in engineering and energy technologies, such as electronics, heat exchangers, and batteries, are allied with heat flux generation, which seriously needs a suitable heat/thermal management system. Conventional fluids have shown constrained applications due to their low thermal conductivity. Therefore, exploring more efficient fluids is becoming a leading development in advanced thermal fluids [2]. To boost the efficiency and heat dissipation of different thermal systems, development in fluid variety is mandatory, especially since various heat-enhancing techniques have failed and practically reached their limits [3] [4]. This key problem spurred the engineering and energy industries to develop advanced thermal fluids with greater thermal conductivity in comparison to conventional fluids (Transformer Oil (TO), Engine Oil (EO), Ethylene Glycol (EG), Water/Distilled water (DW) as explored firstly by Maxwell, Masuda, and Ahuja. Maxwell and Ahuja focused on how to improve the thermal conductivity of conventional fluids using micro-scale metal/nonmetal particles and whether they showed an increase in thermal conductivity after dispersing [3, 5, 6]. Nanofluids are the free suspension of solid nano size particles in a conventional fluid, where the particle diameter should be less than 100nm at varying wt.% or vol% as required. The use of nanofluids in engineering and energy industries is receiving distinct attention from the research community due to their significance for heat transfer improvement; however, some mechanisms need to be completely understood. For many years, the use of metal oxides, graphene,

and carbon based single, hybrid/composites has been investigated for improved thermal properties, where the effect of nanoparticle diameter, especially on thermal conductivity enhancement in nanofluids over a magnetically arranged surface, using Corcinoe's model, showed significant improvement [7] [8]. Similarly, a study reported a comparison of the heat transfer performance of Al_2O_3/H_2O and CuO/H_2O nanofluids over a wedge (a geometry) in aerospace, automotive, and industrial applications such as wings, turbine blades, and heat exchangers. The study claimed that increasing Lorentz forces regulates nanofluid motion over a wedge. Thermal enhancement is observed with higher radiation, Eckert number, concentration, and Biot number, whereas stronger magnetic fields reduce temperature by restricting flow [9]. Another study numerically investigates that Fe_3O_4/EG and $MnZnFe_2O_4$/EG nanofluids over a slanted surface under Cattaneo Christiiv flux, variable temperature, and heat generation. Nanofluid motion is slower than conventional fluid due to density effects. Heat generation and radiation significantly enhance thermal performance, with radiative nanofluids proving more efficient. Shear drag increases with concentration, and Fe_3O_4/EG shows superior heat transport over $MnZnFe_2O_4$/EG [10].

Adnan et al [11] conducted a systematic investigation of multiple nanofluids under Sakiadis flow, revealing that tetra nanofluid (Al_2O_3/MgO/Cu/Ag/H_2O) outperforms hybrid, ternary and simple nanofludis in heat transfer due to its superior thermal conductivity. Thermal radiation, Biot number, and Eckert number significantly enhance thermal performance, with the most pronounced effects for tetra nanofluid. Entropy generation increases with convective heating but is minimized by nonlinear radiation, particularly for tetra nanofluid. These findings establish tetra nanofluid as a promising candidate for high heat industrial applications. Future work may explore gravity, Joule heating, slip effects, and non-Newtonian models for further thermal enhancement.

Iqbal et al [12]. Presented an analytical study on thermal conductivity enhancement using Al_2O_3/water (spherical) based nanofluids. The study includes the use of less than 0.2 vol.% concentration of Al_2O_3 and electrostatic stabilization via pH control, as opposed to steric stabilization with surfactants used for stability control, which are mainly reported to have irregular effects. A notable change was observed in thermal conductivity enhancement for less than 15nm, so it is not necessary to use pH controllers and surfactants to avoid the rise in interfacial resistance. These characteristics indicate that the effects of nanofluid preparation are associated with such physical properties and need to be further investigated. So, the use of pH controllers or surfactants may not be able to achieve such anomalous enhanced thermal conductivity.

Waqar et al [13]. Uses the ZnO-EG@DW based nanofluids for heat transfer, thermophysical, and hydrodynamic characteristics analysis in a square geometry heat exchanger. The ZnO was synthesized via a one-pot Sonochemical technique and confirmed using varying characterizations. Four varying 0.025 wt.%, 0.05 wt.%, 0.75 wt.% and 0.1 wt.% of ZnO-EG@DW based nanofluids were prepared using a 2-step nanofluid preparation technique. All the wt.% concentrations were tested for thermal conductivity measurements starting from 20 ºC to 45 ºC, and a linear enhancement was found with an increase in temperature and wt.% of ZnO. Further Heat transfer improvement in square geometry was tested using the Reynolds range from 5849 to 20,360 at varying wt.% concentrations. A significant enhancement was noticed at higher wt.% and greater values of the Reynolds number. A few more similar studies were conducted by the same author using ZnO/DW at the same wt.% concentrations and different geometries of heat exchangers, and reported significant outcomes.

Sajid et al [14]. Prepared CuS-ZnO/water based nanofluids at 0.005 and 0.0025 mass% via a well known 2-step technique with 5 % of ZnO and 95 % of CuS. These nanofluids were used to reduce

the cooling transmission load of a greenhouse roof in agriculture, where the visible spectrum was transmitted and absorbed by the solar spectrum and infrared radiation. Both concentrations, particle size, and optical stability within visible and infrared regions were evaluated here using 2-hollow ducts with 4mm and 8mm thickness. These 2 ducts are related to a greenhouse setup and are kept in front of the solar simulator. The key outcomes showed that using CuS-ZnO/water caused a decrease in the internal temperature of the greenhouse at ambient temperature. When CuS-ZnO/water nanofluids were flowing through an 8mm duct, 27.4% less internal heat was achieved inside the greenhouse unit in comparison to no fluid used. Similarly, a greater 82.2% positive crop growth was seen by using an 8mm duct. Overall, the 0.42-year payback period of these nanofluids was reported in the study for the 8mm duct.

Ehsan Raki et al [15] conducted a study to see the effects of the magnetic field on heat transfer using cobalt oxide (Co_3O_4) and deionised water-based magnetic nanofluids. The significance of the current study exposes the use of Co_3O_4 (45nm size) dispersed in deionized water based nanofluids at 0.2, 0.1, 0.05, 0.01, and 0.005% volume fractions as a nucleate boiling device. The experimental trials revealed an increase in surface heat resistance and deposition with a rise in the volume fraction of cobalt based nanofluids, which caused a decrease in the nucleation and boiling heat coefficient. Similarly, the magnetic field has shown positive effects on the nanofluids, which led to a negative effect of the magnetic field on more concentrated nanofluids. In light of these statements, a significant improvement of 58 % in heat transfer of pool boiling due to a magnetic field was recorded at a low 0.005% volumetric concentration of Co_3O_4/DI-water nanofluids as compared to pure DI water fluid. A few more similar studies were conducted to study the heat transfer and thermal conductivity changes using pure liquid and varying nanofluids like (NiO-based/water, MWCNTs-SiO_2/Water-EG, and Silica/deionized water) at varying volumetric

concentrations, with and without using magnetic fields. All of these studies reported significant outcomes of nanofluids when compared with pure liquid results[16-18].

Waqar et al [19] reported on the use of metal oxide based binary composite nanofluids of ZnO and TiO_2 Sonochemically dispersed in distilled water at 0.025 wt.%, 0.05 wt.%, 0.75 wt.% and 0.1 wt.% concentrations for the heat transfer, thermophysical and hydrodynamic studies of square shape pipe. A significant increase in thermal conductivity (TC) of 47% was reported in the study, which is mainly credited to the higher wt.% and greater temperature value. The overall 57% improvement in average heat transfer (HT) was recorded at 0.1 wt.% concentration and a higher flow rate. Finally, the study claimed a more effective combination of ZnO and TiO2 binary composite that caused a significant enhancement in both TC and HC. Another study was reported by the same author using a circular geometry of a heat exchanger, the same nanofluids, the same wt.% concentrations and different Reynolds numbers; this study also showed prominent outcomes of using binary composite nanofluids.

Many studies were executed in the past on using single and hybrid nanofluids for thermal conductivity and heat transfer enhancement related applications, and were found to be a potential agent in thermal management systems. The metal oxide based binary composite or hybrid nanofluids showed surprising enhancements in both (TC) and (HT) as compared to conventional fluid and single nanofluids. Leading to the same idea, we tried here to use the 3 different metal oxides sonochemically dispersed in a mixture of EG@DW and to see the effects on all thermophysical, thermal, and hydrodynamic characteristics while using a circular heat pipe.

1.1. KEY OBJECTIVES

The following are the key objectives of the current experimental study.

- Preparation of Mixed metal oxide based MMO/EG@DW ternary hybrid nanofluids (THN).
- Study of thermal conductivity enhancement after adding 3 different metal oxides.
- Study of the effects of mixing different metal oxides on the thermophysical characteristics of THN.
- Study of heat transfer improvement using THN prepared using EG@DW.
- Analysis of Local/Average Heat transfer coefficient and Nusselt number improvement using THN.

1.2. MATERIALS AND METHODOLOGY

1.2.1. Materials

Zinc $ZnC_4H_6O_4$ as a precursor and NaOH as a strong acid for a chemical reaction to produce ZnO were procured from Sigma-Aldrich. The commercially available Al2O3 and TiO2 were also procured and used for THN preparation. Ethylene glycol 99.9% purity and distilled water were used for chemical reactions and other washing purposes. All the chemicals were of analytical grade and certified.

1.2.2. Methodology

The mixed metal oxide dispersed in ethylene glycol and distilled water (MMO/EG@DW) based ternary nanofluids (THN) are prepared via a broadly used facile 2-step preparation technique. This technique easily allows control over the mixing ratios of the single/hybrid particles. Fig.1 shows that in Step 1, the ZnO was prepared using its precursor (Zinc Acetate, NaOH, EG, and DW) as raw materials. The ZnO was synthesized via the Sonochemical method and confirmed by varying characterizations like XRD, FTIR, EDX, FESEM, UV-vis, TEM, etc. The ZnO average size was attained up to 17nm, and most particles were spherical in shape. In Step-2, again, the

ultrasonochemical nanofluid preparation technique was adopted to prepare MMO/EG@DW based THN. The high-power probe sonicator with prior functional and control settings was used for particle dispersion. Firstly, the synthesized ZnO (33.3 % of the total MMO) nanoparticles were dispersed in a mixture of both EG and DW (50:50) under probe sonication for 20 minutes. The EG and DW mixture was prepared using a magnetic stirrer for 20 minutes. Further, two metal oxides, Al_2O_3 and TiO_2, were added physically (33.3 % of each of the total MMO) into the ZnO/EG@DW solution and stirred. This stirring process was continued until all metal oxides were mixed in the EG@DW mixture. Then this solution was placed in a probe Sonicator to sonicate it; a maximum of 2 hours was chosen to sonicate the solution. The Sonicator's functional and operational controls were adjusted before starting it. The pulse time was 3/2 on-off, maximum pulse energy was 360,0000J, the pulse amplitude was 70, the Probe temperature was 0, the power was 750 watts, and the input voltage was 220. The MMO/EG@DW based THN was prepared at 4 varying wt.% concentrations: 0.025 wt.%, 0.05 wt.%, 0.075 wt.%, and 0.1 wt.%. The same preparation process was adopted for each wt.% concentration. Finally, we obtained well dispersed and stable MMO/EG@DW based THN, which was later tested for stability and other thermal analysis studies.

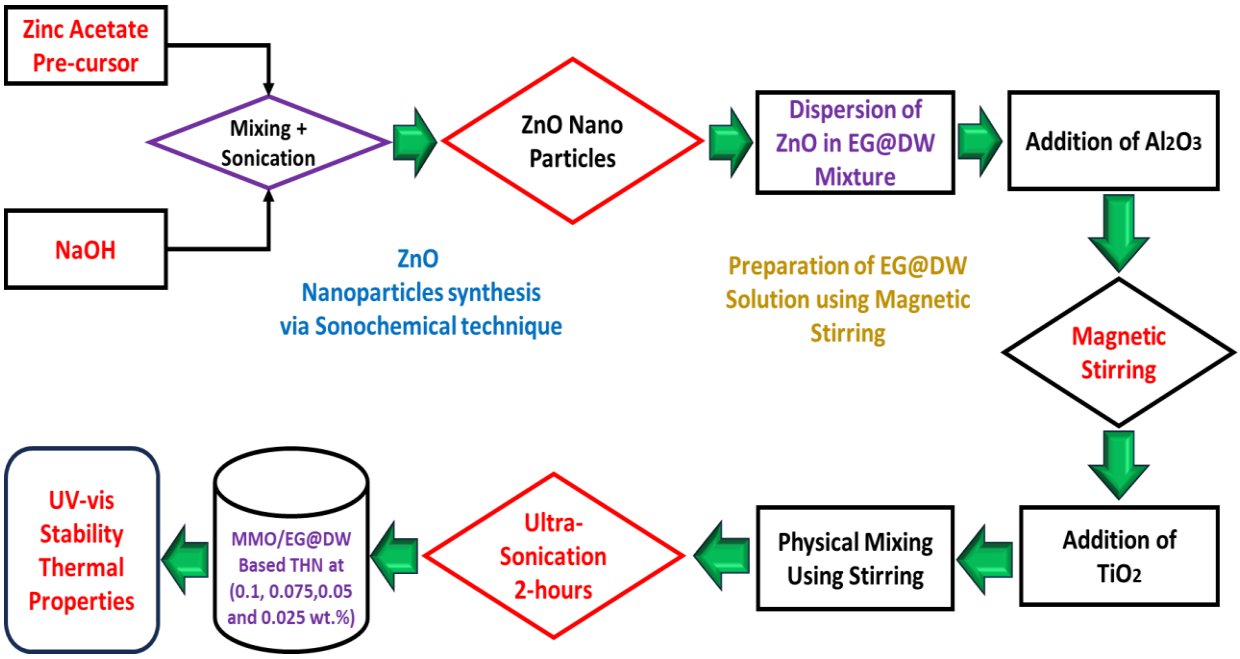


Fig.1 Ternary Hybrid Nanofluids (THN) preparation flow.

1.3. EXPERIMENTAL SETUP

A fully calibrated heat transfer measurement system consists of a storage tank (Liquid/Nanofluid) of 12L maximum, flow pump, pre-heating part, control valves, flow bypass pipe, condenser, liquid chiller, circular test section (1.2m length and 0.01m internal diameter), five K-type thermocouples, inlet temperature thermocouple (Tin), outlet temperature thermocouple (Tout), digital flow meter, digital data logger, pressure transducer, control panel, voltage regulator and glass wool insulation as shown in Fig.2a and Fig.2b. The test section is made of a smooth copper tube on which thermocouples are attached vertically apart from each other with 0.2m as given in Fig.2c. These thermocouples are attached with a pipe surface using a capped jacket around them and a small grove on the surface. Further, all the thermocouples have been directly connected to the digital data logger. This circular tube pipe is coiled with a heating wire of 220W around the test section to provide external heating effects. The total active length (heating area) is 1m and fully wrapped with insulated glass wool of at least 4cm thick to save heat losses from the pipe surface. Finally,

this insulated pipe is again wrapped with aluminium foil to avoid further heat losses. Many other functional controls have been used to fully calibrate and organize experimental setups, like flow control, inlet control, temperature control, fluid exit valve, velocity control, pump frequency control, heater power control, etc. The presented experimental setup is fully optimized and has been used for a long time for experimental studies. The following testing equipment and their associated conditions were considered, as given in Table 1.

Table 1 Specifications and accuracy of the devices and sensors used in experimentation

Parameters for Measurement	**Device/Sensor Type**	**Overall Working Conditions**	**% Error**
Heat Exchanger Surface Temperature	Highly Sensitive K-Type Thermocouples	0 °C to 300 °C	± 0.12
Bulk (Tb) temperature	RTD Sensors (PT/100)	0 °C to 200 °C	± 0.1
Flow meter	Paddlewheel (Burket Ceramic)	0.031 to 12 m/s	± 0.5 %
Pressure Drop/loss	Pressure Transducer (ALIADP)	0 to 25 kPa	± 0.076 %
Cooling Unit	Refrigerated cooling bath (WISECIRU DAHIHAN)	2.2 kW	± 0.1
Power Supply	Voltage and Ampere	220V	± 0.1
Multimeter	Voltage, Current, Resistance	AC/DC	± 0.1

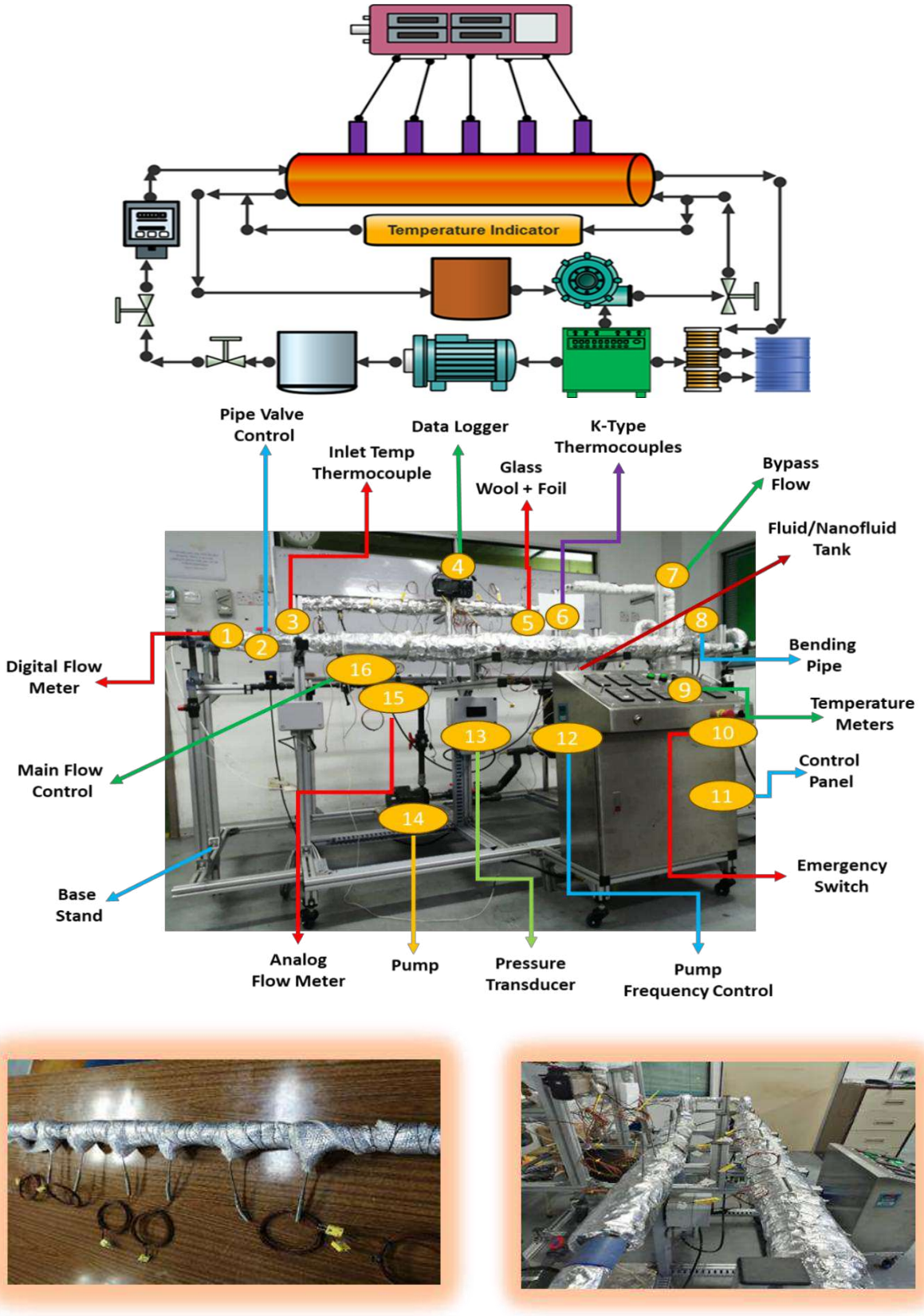


Fig.2 a) Heat transfer test rig schematic, b) Pictorial view and c) Circular heat exchanger

1.4. Data Analysis

The following mathematical models, given in Eq.1 and Eq.2, were used to evaluate thermal conductivity changes at varying temperatures and wt.% [20] [21].

$$\frac{keff}{kf} = ks + 2kf + 2\emptyset\frac{(kf-ks)}{} ks + 2kf - \emptyset(kf - ks) \quad (1)$$

$$\frac{keff}{kf} = kp + (n - 1_{kf} - (n-1)(kf - kp)\emptyset / kp + (n-1)kf + (kf - kp)\emptyset \quad (2)$$

Eq.3 was used to analyze the (h), where q is the value of heat flux, Tw is the value of wall/ surface temperatures, and Tb is the bulk temperature. Tb could be calculated by using Newton's cooling law.

$$h = \left(\frac{q''}{Tw-Tb}\right) \quad (3)$$

The Heat flux was measured by analyzing the total area and delivered power for the flow passage, where Q is the total power (V*I) applied to the heater, and A is the value of the total surrounding area shown in Eq.4.

$$q'' = \left(\frac{Q}{A}\right) \quad (4)$$

Eq.5 was used to measure the area of the square heat exchanger for further heat transfer analysis.

$$A = 4AL \quad (5)$$

The 600 watts of heating power was applied externally to the heat exchanger using a heater, and Equ 6 was used to calculate the Nusselt (Nu) values. Where (h) is the value of the heat transfer coefficient, D_h is the hydraulic diameter of the square heat exchanger, and k is the value of the thermal conductivity. In addition, for single nanofluids, Petukhov [22] and Gnielinski[23] have projected different correlations. This way, the following equations 6-10 were used to evaluate Nusselt (Nu) values accordingly.

$$Nu = \left(h * \frac{D_h}{K}\right)$$

(6)

Further, Eq.7 was used to calculate Reynolds' values. Here, ρ represents the density, v represents the velocity, μ represents the viscosity, and D represents the internal diameter of the heat exchanger.

$$Re = \left(\frac{\rho v D}{\mu}\right) \tag{7}$$

$$Nu = \left(\frac{\left(\frac{f}{8}\right)(Re-1000)Pr}{1++12.7\left(\frac{f}{8}\right)^{0.5}(\mathrm{Pr}\,\hat{}\,2/3\ -1)}\right) \tag{8}$$

$$Nu = \left(\frac{\left(\frac{f}{8}\right)RePr}{1.07+12.7\left(\frac{f}{8}\right)^{0.5}(\mathrm{Pr}\,\hat{}\,2/3-1)}\right) \tag{9}$$

$$Nu = (0.023Re^{0.8}\ \mathrm{Pr}^{0}.4) \tag{10}$$

Eq.11 and Eq.12 were used for the calculation of the friction coefficient presented by Petukhov[22] [24] [25], where f is the friction loss, ΔP is the pressure variation, L is the whole length of the heat exchanger, D is the diameter, ρ is the density, and v denotes the velocity.

$$f = (0.79LnRe - 1.64)^{-2} \tag{11}$$

$$f = \frac{\Delta P}{\left(\frac{L}{D}\right)\left(\frac{\rho v^2}{2}\right)} \tag{12}$$

$$f = 0.3164re^{-0.25} \tag{13}$$

The pumping power required by the system for the turbulent flow in a square heat exchanger was measured using the following Equ 15 [26], where the Reynolds values were kept constant.

$$W = 0.158\left(\frac{4}{\pi}\right)^{1.75}\left(\frac{Lm^{2.75}\mu^{0.25}}{\rho^2 D^{4.75}}\right) \tag{14}$$

$$\frac{Wnf}{Wbf} = \left(\frac{\rho bf}{\rho nf}\right)^2\left(\frac{\mu nf}{\mu bf}\right)^3 \tag{15}$$

2. RESULTS AND DISCUSSION

2.1. MMO ternary Hybrid Material FESEM Characterization

Although the FESEM image does not provide any relevant details about the functional groups that may form during mixing of the MMO to prepare ternary hybrid nanofluids (THN), this characterisation clearly shows uniform mixing and particle morphology, providing evidence of successful ternary hybrid material preparation. Fig. 3 illustrates the FESEM image of combined mixed metal oxides (MMO), in which Al_2O_3, TiO_2, and ZnO of different sizes and shapes were sonochemically mixed in equal ratios of 33.3% each. The commercially available Al_2O_3 and TiO_2 were procured from Sigma-Aldrich, and ZnO was self-synthesised. For the FESEM imaging of the MMO ternary hybrid material, high resolution machines were used, where MMO powder was placed on the carbon electrode and put under testing. A chunk of 500 μm of MMO was taken for morphology testing, considering these parameters: 10.00kV, mag 200,000x, ETD, WD=5.1 mm, and High vacuum (vacMode). Finally, FESEM analysis revealed a heterogeneous morphology comprising three distinct particle geometries: spherical, prismatic/rectangular, and cylindrical structures, corresponding to the respective metal oxide constituents.

2.2. MMO ternary Hybrid Material UV-Vis Analysis

UV-vis spectroscopy is a typical method used for the investigation of the nanoparticle's stability and dispersion in a base liquid. The Beer-Lambert principle states a direct relation between the wt.% concentration of the absorbing substance (Nanoparticles) in a liquid and colloidal suspension. Pursuing this law, the absorbance spectrum of all metal oxides, individually and together, showed different peaks according to the $\pi - \pi$ interaction of a conjugated system. The UV-vis spectrum analysis was executed using the SHIMADZU machine to study the optical behaviour of ZnO, Al_2O_3+TiO_2, and Al_2O_3+TiO_2+ZnO (MMO) dispersed in a mixture of

EG@DW. Fig.4 depicts the UV-vis spectra of all metal oxides individually and all together. All the metal oxides showed different absorbance peaks at different wavelengths. The absorbance peak for all three MMOs was located at 2.75 %, while the peak for Al_2O_3+TiO_2 and single ZnO was located near 2%, which could be due to the wt.% concentration difference. Because there is a direct relationship between absorbance and wt.% concentrations of the loading particles, which satisfies the Beer-Lambert law.

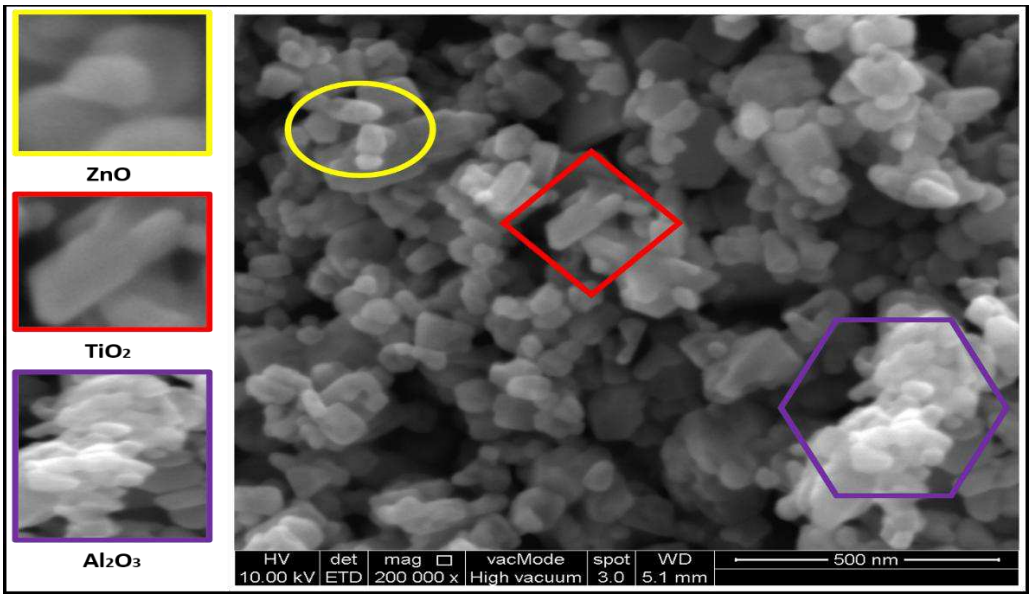


Fig.3 FESEM analysis of Ternary Hybrid Nanofluids (THN).

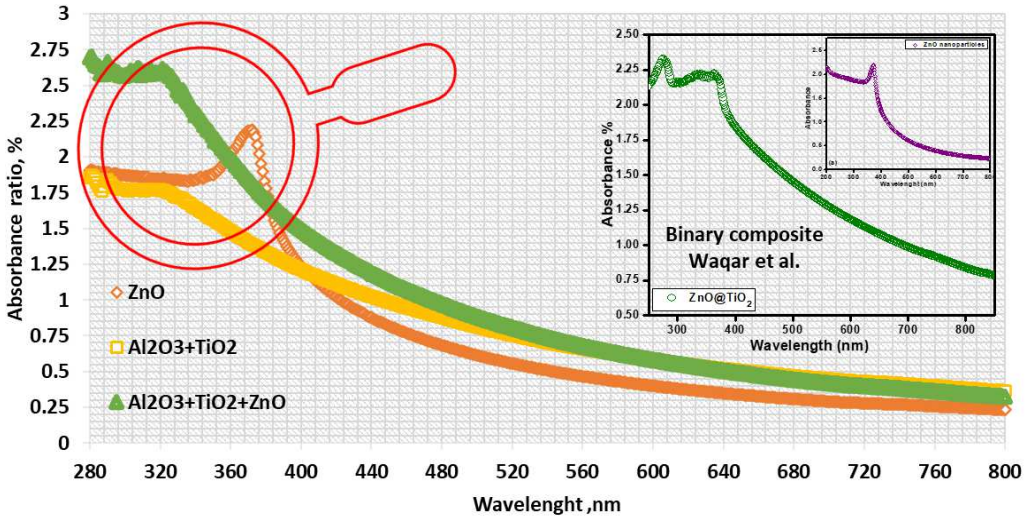


Fig.4 UV-vis analysis of Ternary Hybrid Nanofluids (THN), single, binary and ternary.

3. Dispersion and Stability

The stability of nanofluids over a long time is the critical criterion for their use as a storage source and for improving further thermal properties [27]. Various techniques have been experimented with to verify the nanofluids' dispersion and stability. A few of them are the Visual method, Zeta potential technique, Dynamic light scattering, Photometry, absorbance % method, and sedimentation photographs method. Other than these techniques, the different thermophysical characteristics like specific heat, viscosities, thermal conductivity, and thermal diffusivity over the time span could also be used to measure the stability of nanofluids [28] [29]. All the mentioned techniques have their advantages and disadvantages based on their usage and applications. Similarly, various stability-enhancing techniques like (Physical method, High Sonication, Magnetic stirring, High shear stirring, Chemical method, using surfactants or stabilizing agents, surface functionalization, and pH changing) could be used to get longer suspension of solid nanoparticles dispersed in varying nanofluids. In the current study, the sedimentation photograph method has been adapted for better observation of nanofluids' stability, and the high-probe sonication method was used to get uniform and equal dispersion of all MMO in the base fluid (EG@DW). This method is also called the visual technique, where the prepared nanofluids were kept stable/steady in transparent glass bottles or jars without any external disturbance. Then these nanofluids need to be observed regularly for a specified time to see the sedimentation of solid particles. The greater sedimentation of solid particles caused to change in the nanofluid color which will be most likely to the base fluid and will be considered as an unstable state.

Fig.5 portrays the stability analysis of all wt.% concentrations of MMO/EG@DW based THN without using any surfactant or stability enhancing agent since the day of preparation. As mentioned above, the visual or sedimentation photograph method was adapted to assess stability.

All the photographs depict the stability and sedimentation behaviour of all nanofluids. Photographs clearly show that all nanofluids were well stable and suspended for 6 weeks, where no sedimentation happened or maybe very, very little since the day of their preparation. From week 7, it can be seen that the nanofluids started to change their colours, which meant sedimentation was happening. The sedimentation ratio is not the same for all wt.% concentrations; it was higher for the lower 0.025 wt.% concentration, while lower for the higher 0.1 wt.% concentration. The evidence behind this longer suspension could be the viscosity of the base fluid (EG@DW), which is higher than DW and the high probe sonication of all the MMO highly dispersed in the base fluid. This is an achievement of getting stability for up to 6 weeks, especially when using different metal oxides and without using any surfactant or stabilizing agent, because many studies have reported the negative impact on thermal conductivity while using surfactants.

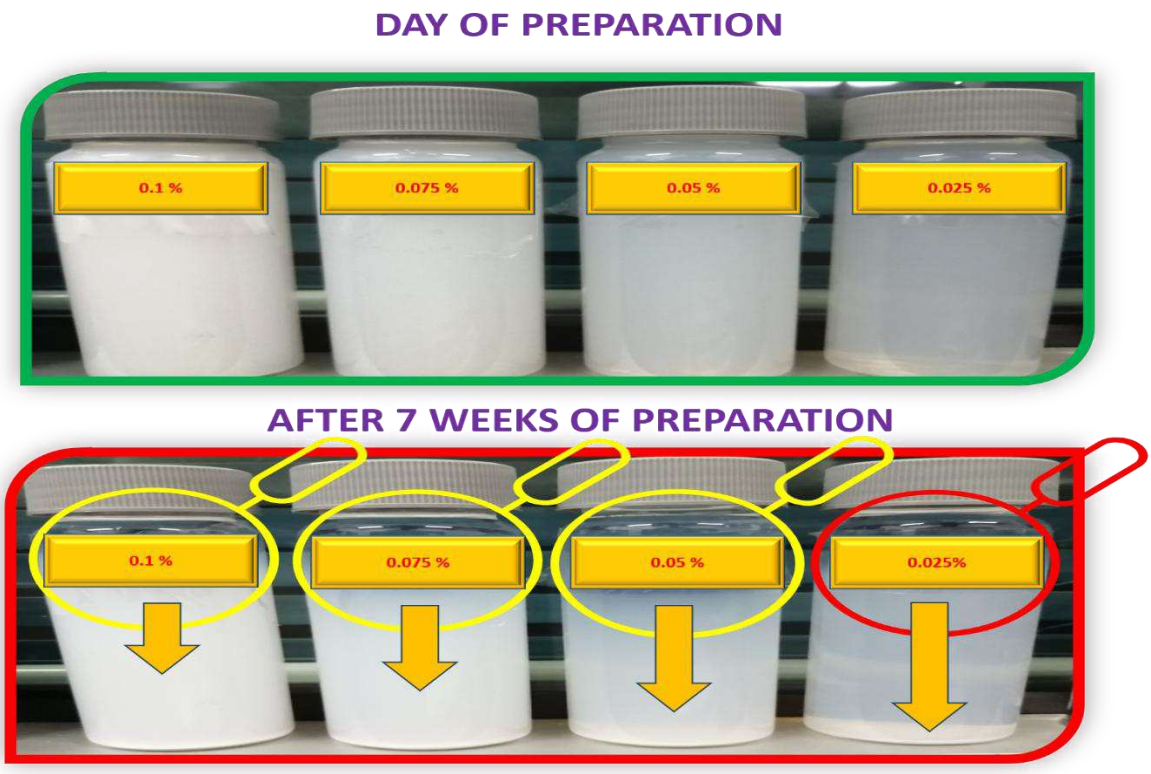


Fig.5 Stability and sedimentation analysis of Ternary Hybrid Nanofluids (THN).

4. Thermophysical Properties of MMO/EG@DW based Ternary Hybrid Nanofluids

The temperature values have a significant impact on the fluid/nanofluids viscosities, where they can play a substantial role in the existence of nano size particles and their respective wt.% concentrations. Consequently, it is important to find out the significant effects of adding nano size particles on the viscosity of fluids against varying temperature values [30]. Fig.6a and Fig.6b depict variations in kinematic and dynamic viscosity against temperature changes, where it can be seen that the temperature changes showed a greater influence on changing the viscosity values. The temperature rise caused an increase in molecular motion and decreased dynamic viscosity and van der Waals forces. Another key reason for the rise in viscosity is the addition of more solid particles into the base fluid. The vol.% or wt.% fraction caused changes in both dynamic and kinematic viscosities, which is attributed to interaction forces and intermolecular forces between the nanoparticles. These forces create resistance during the movement of the particles in the base fluid, which further leads to an increase in viscosity.

4.1. Kinematic/Dynamic Viscosities of MMO/EG@DW based THN

The current experiments show that at a 100rpm shear rate and temperature changing from 20ºC to 45ºC, the kinematic viscosity and dynamic viscosities of MMO/EG@DW based THN start to change with temperature changes. The temperature influence on these nanofluids at varying wt.% concentrations is illustrated in Fig.6a and Fig.6b. It can be seen that a significant decrease in both viscosities occurred at all wt.% of MMO/EG@DW based THN compared with 20ºC, 25ºC, 30ºC, 40ºC, and 45ºC temperatures. The higher viscosities were recorded at 20 °C and 0.1 wt.% concentrations as compared to 45 °C and at all other wt.% concentrations. Similarly, the maximum drop in both viscosities was recorded at higher temperatures and a lower 0.025 wt.% concentration

of MMO/EG@DW based THN. This decrease in both viscosities is mainly due to the temperature, which caused the gain of energy and mobility of all three mixed metal oxide (MMO) solid nanoparticles, which may be caused by a decrease in agglomeration. At low temperatures, these nanoparticles absorb less energy, and their intermolecular forces become weaker owing to temperature [31].

4.2. Density of MMO/EG@DW based THN

A digital density meter of the DMA 4100/M model was used to measure the densities of base fluids EG@DW and MMO/EG@DW based THN. The density meter was adjusted for the temperature function, along with prior calibrations, to utilize base fluids and nanofluids at different temperatures. The density was calculated for all wt.% concentrations, and the base fluid was varied from 20 ºC to 45 ºC with an equal interval of 5 ºC, where each reading was repeated at least 5 times, and an average value was considered. The overall density meter uncertainty was about 0.02%.

All prepared MMO/EG@DW based THN and base fluid EG@DW were investigated for density measurement against different temperature values: 20 ºC, 25 ºC, 30 ºC, 35 ºC, 40 ºC and 45 ºC temperatures repeatedly. Fig.6c presents the changes happening for wt.% concentrations against temperature variations. Firstly, the mixture of EG@DW is tested for all temperature values to check the experimental accuracy and measurement accuracy. It can be seen that the lower 0.025 wt.% concentration density is almost near the base fluid (EG@DW) for all temperature values. But as the wt.% concentrations increased, the overall densities of all nanofluids started to increase, while, on the other hand, they started to decrease with the temperature. All the fluids and THN showed a declining trend with the increase in temperature. At higher temperatures, 45 ºC, the density of all wt.% concentrations and the base fluid seems very low. The density is the key

parameter that has a significant effect on the friction factor, pressure loss, Nusselt numbers, and Reynold numbers. In the current study, the highest density of 1.078 g/mol of MMO/EG@DW based THN was noted at 0.1 wt% at a lower 20ºC temperature, while it decreased to 1.508 g/ml of the same wt.% at a 45ºC temperature value. In comparison, a similar trend was reported in the previously published literature [32] [33].

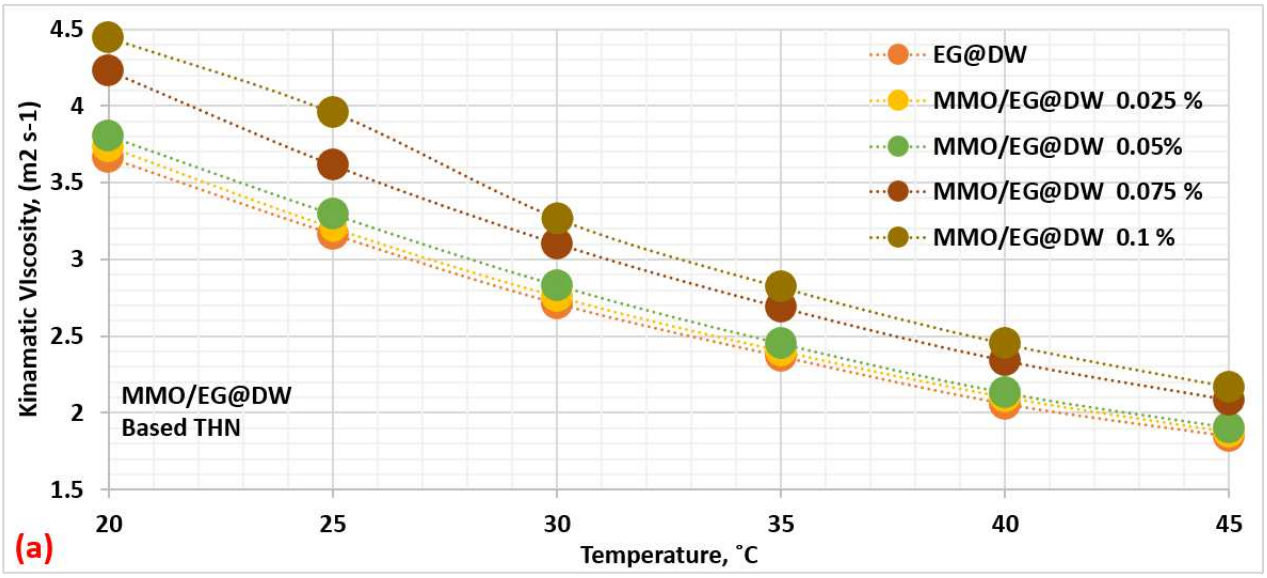
4.3. Thermal conductivity of MMO/EG@DW based THN

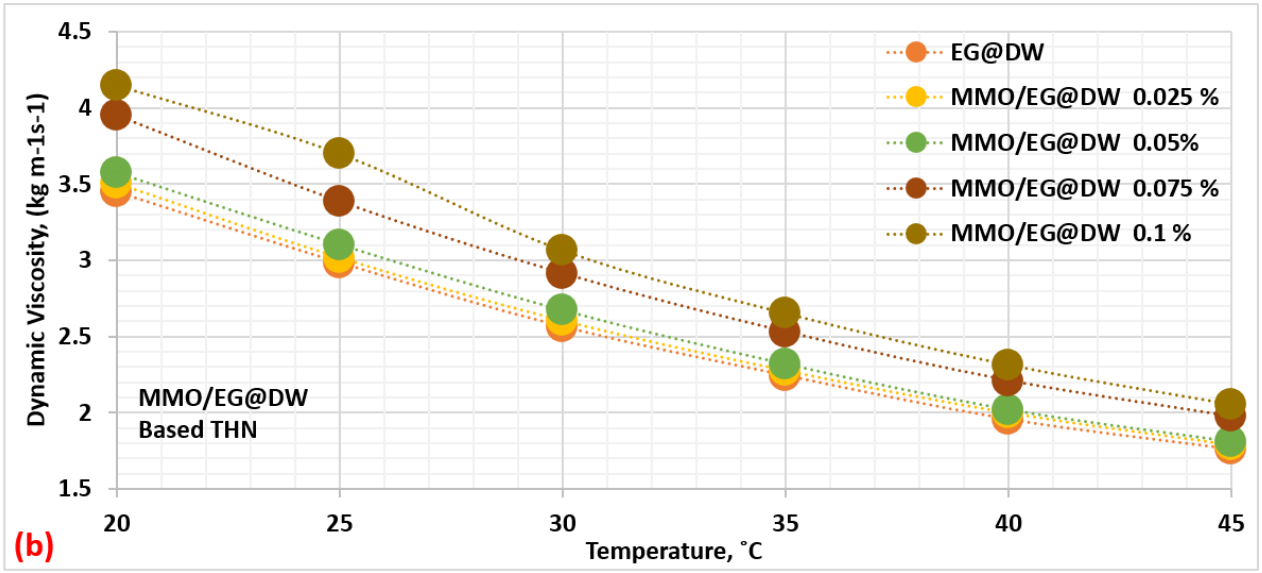
Numerous kinds of solid nanoparticles can be utilized to prepare varying nanofluids, where metal oxides are considered more promising and have been used in different conventional fluids [34] [35] [36]. Aberroundmand et al [37]. Comprehended an experimental approach to finding the thermal conductivity of CuO-engine oil based nanofluids to see how the varying 0.2 wt%, 0.2 wt%, 0.5 wt%, and 1 wt% concentrations affect thermal conductivity while varying temperatures were employed. At a 1 wt.% concentration of the same nanofluid, a total 49% improvement in the thermal conductivity was achieved, which confirmed that the addition of solid nanoparticles caused an increase in the thermal conductivity of base fluids [38]. Similarly, the particle shape and size mainly affect the overall thermal conductivity of varying nanofluids. This particle size is similar to the rise in temperature and influences the collision of particles; therefore, it is a key factor affecting thermal conductivity [39]. Plenty of studies have reported on the particle size effects on the change in thermal conductivity of all kinds of nanofluids [40].

Alawi et al [41] conducted a study on the shape effects of varying particles on the thermal conductivity of nanofluids, where they used SiO_2/W, Al_2O_3/W, ZnO/W and CuO/W metallic based different nanofluids. The study reported that improved thermal conductivity depends on both the best particle shape and the type of nanoparticles. Similarly, Waqar et al [42] conducted studies on the use of single and composite metal oxide based nanofluids of ZnO/Dw, ZnO/EG@DW, and

$ZnO+TiO_2$/DW for varying thermal properties analysis, including thermal conductivity. All these studies showed that the addition of solid particles, particle size, and particle shape caused changes in thermal conductivity when tested at different temperatures. Further studies revealed that mixing different types of particles gives more enhanced thermal conductivity as compared to using single particles. At 0.1 wt.% concentration of binary composite of ZnO+TiO2/DW based nanofluids showed greater thermal conductivity and other properties [19, 43].

Considering all past studies on thermal conductivity enhancement, the current experimental work has led to measuring thermal conductivity improvement of four varying 0.025 wt.%, 0.05 wt.%, 0.075 wt.%, and 0.1 wt.% concentrations of MMO/EG@DW based THN nanofluids. The reference temperatures of 20 °C, 25 °C, 30 °C, 35 °C, 40 °C, and 45 °C have been considered to measure the thermal conductivity changes at varying wt.% concentrations. For the base fluid (EG@DW) and all other wt.% of MMO/EG@DW, the same temperature ranges have been used. Fig.6d represents all the changes that happened during the thermal conductivity measurement of all samples. It can be seen that the base fluid (EG@DW) showed the least improvement in thermal conductivity at all temperature values. This behaviour is clear evidence of nanoparticle absence of nanoparticles, while in the same spectra, all other samples showed improved thermal conductivity, which indicates the presence of MMO addition. The addition of MMO led to higher thermal conductivity, while a lesser addition contributed to lower improvement. A substantial augmentation was recorded at a higher 0.1 wt.% of MMO/EG@DW based THN and a 45°C temperature value. The greatest improvement of 1.24 W m-1K-1 was attained at 0.1 wt.% concentration. Similarly, all other wt.% also showed respective improvements in thermal conductivity.


Kinamatic VIscosity, (m2 s-1)
4.5
4
3.5
3
2.5
2
1.5
20
25
30
35
40
45
Temperature, ˚C
EG@DW
MMO/EG@DW 0.025 %
MMO/EG@DW 0.05%
MMO/EG@DW 0.075 %
MMO/EG@DW 0.1 %
MMO/EG@DW
Based THN
(a)


Dynamic Viscosity, (kg m-1s-1)
4.5
4
3.5
3
2.5
2
1.5
20
25
30
35
40
45
Temperature, ˚C
EG@DW
MMO/EG@DW 0.025 %
MMO/EG@DW 0.05%
MMO/EG@DW 0.075 %
MMO/EG@DW 0.1 %
MMO/EG@DW
Based THN
(b)

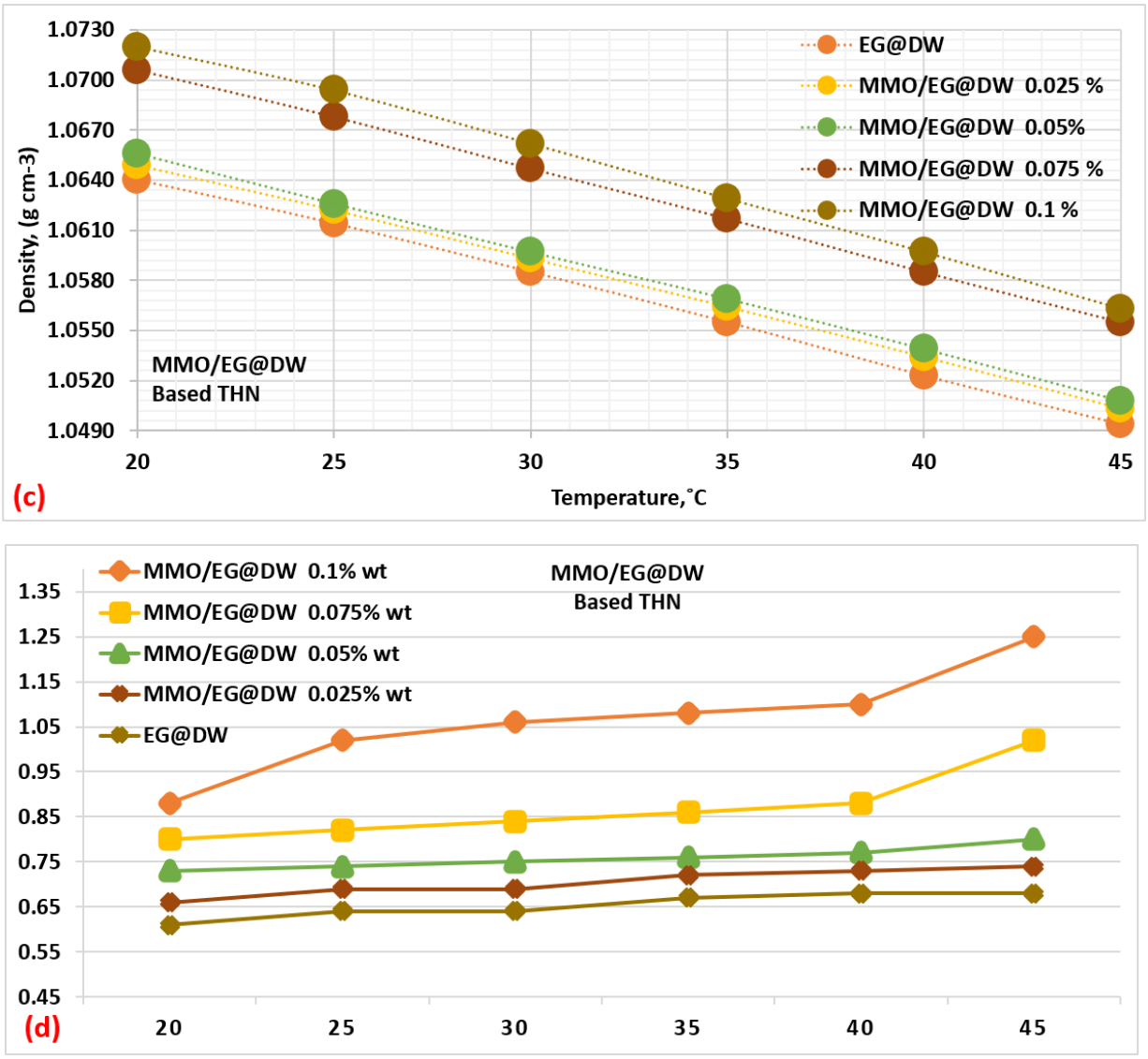


Fig.6 **a)** Kinematic viscosity measurements of EG@DW and all wt.% concentrations of Ternary Hybrid Nanofluids (THN), **b)** Dynamic viscosity, **c)** Density and **d)** Thermal Conductivity.

5. Average Heat Transfer Coefficient, CHTC and Average Nusselt Number (Nu) Measurements of MMO/EG@DW based THN in a Pipe Heat Exchanger

Before starting the experiments with nanofluid, the verification of the experimental system was carried out using distilled water as a reference fluid, where the consistency of all calculations was tested. The sensitivity of the thermocouples and their accurate operation were also examined

before starting the experiment. All the experiments were executed at room temperature. The convective heat transfer (CHTC) measurement was considered in the current study in the turbulent flow regions using Reynolds (Re) varying from 5849 to 24544, where MMO/EG@DW based THN with equal addition of all metal oxides ZnO, TiO_2 and Al_2O_3 nanoparticles at four varying concentrations of 0.025 wt.%, 0.5 wt.%, 0.075 wt.% and 0.1 wt.% concentrations were run one by one using a heat transfer test rig for the heat transfer improvements. The 615W of electric power was adjusted for the test rig, and the constant temperature of 30 °C was maintained at the inlet point. Both average and local heat transfer were measured for EG@DW base fluid and all wt.% concentrations against the same Reynold values. Fig.7a shows the development of average CHTC, where it can be seen that there is an increase in the Reynold values (Re) for both the base fluid and THN. The addition of solid nanoparticles and a hybrid combination of metal oxides with a mixture of EG@DW based fluid showed a significant impact on CHTC enhancement. The base fluid offered a lower enhancement in CHTC, which is due to the absence of MMO nanoparticles. The utmost enhancement was detected at a higher 0.1 wt.% concentration of MMO/EG@DW based THN, while all other 3 wt.% concentrations also showed enhancement in CHTC, respectively.

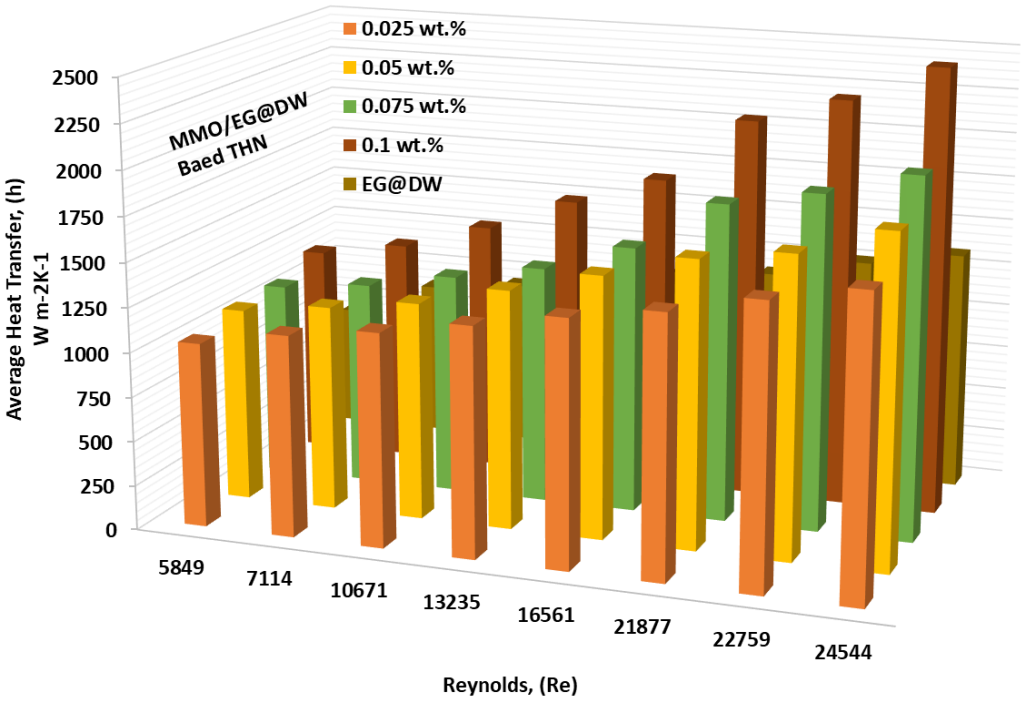
This key enhancement in CHTC of MMO/EG@DW based THN is due to the thickness reduction of the thermal layer and augmented thermal conductivity of the nanofluid in the presence of MMO, which caused a plummeting in the thermal resistance between the nanofluid and pipe (Heat Exchanger) walls compared to the EG@DW base fluid [44] [45] [46]. Similarly, the specific area of solid MMO particles and Brownian motion also influence an increase in CHTC in the current study.

The average Nusselt (Nu) numbers were obtained from the experiments conducted by the same author, Waqar et al. [47], where he compared the data coming from the (DW, EG@DW, EG) base

fluid with different empirical correlations of Gnielinski et al. [48], Dittus-Boelter et al. [49] and Petukhov et al. [24]. The outcomes depicted a rise in Nusselt numbers (Nu) while Reynold numbers (Re) increased. In addition, all relevant experiments and their outcomes showed great consistency with results that came from empirical correlations. The average errors of 7.1%, 7.6 %, and 2% between experimental data and the model's data were examined during the execution of the experiment and its analysis. Therefore, the results from the analysis showed a strong relationship between experimental outcomes and model data, and the error was not >10%. This is all due to the well optimized and precise setup for the CHTC measurements. Hence, the same setup is well suitable and acceptable for further explorations of different nanofluids.

To appraise the convective to conductive heat transfer of MMO/EG@DW based THN, the average Nusselt numbers (Nu) were obtained using Eq.6, which are based on the value of "h" as presented in Fig.7b against the different Reynolds numbers (Re) and at varying 0.025 wt.%, 0.5 wt.%, 0.075 wt.% and 0.1 wt.% concentrations. It can be seen that all the fluids and nanofluids showed a significant increase in Nusselt numbers (Nu) with the rise in Reynold (Re) values. Similarly, this increase in Nusselt numbers (Nu) is also happening due to the increase in wt.% of all ternary hybrid nanoparticles. Similar to the highest rise in CHTC, the rise in a greater increase in Nusselt numbers (Nu) was recorded at a higher 0.1 wt.% of MMO/EG@DW based THN nanofluids and 24544 Reynolds (Re), which are far greater than a single EG@DW base fluid. All other wt.% concentrations also contributed significant enhancement in Nusselt numbers (Nu) across all Reynolds (Re). This improvement in Nu is mainly ascribed to the Brownian motion, thermophysical characteristics and surface area of the well dispersed and suspended MMO, which further improves the energy transportation ability of the nanofluids. In addition, one reason behind this improvement in Nu could also be lower specific heat and higher thermal conductivity when

compared with the pure EG@DW base fluid. Fig.7c represents a comparison between current outcomes and varying correlations presented by different authors; a very close and reliable relationship was found in the current data, and outcomes come from correlations.



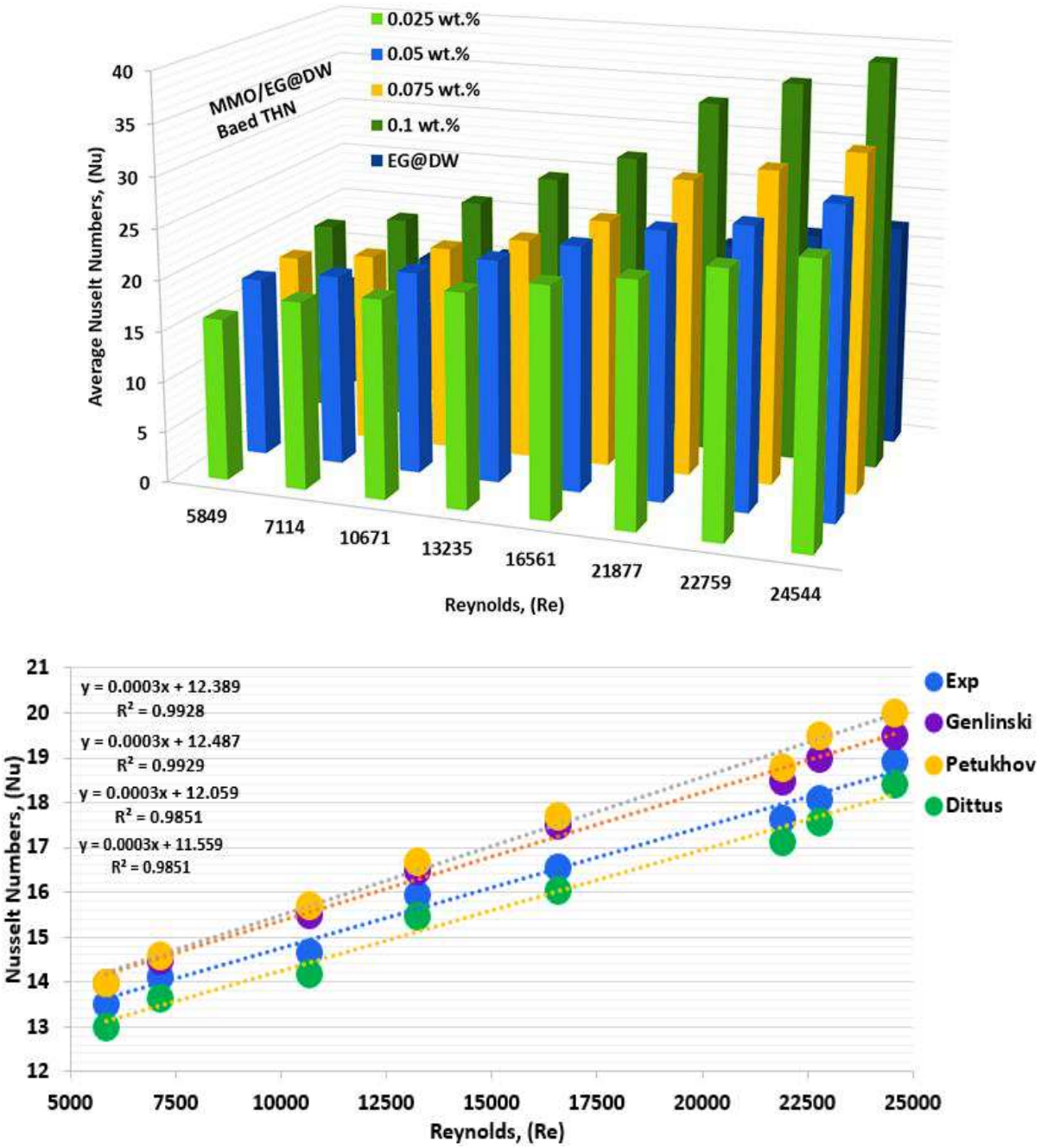
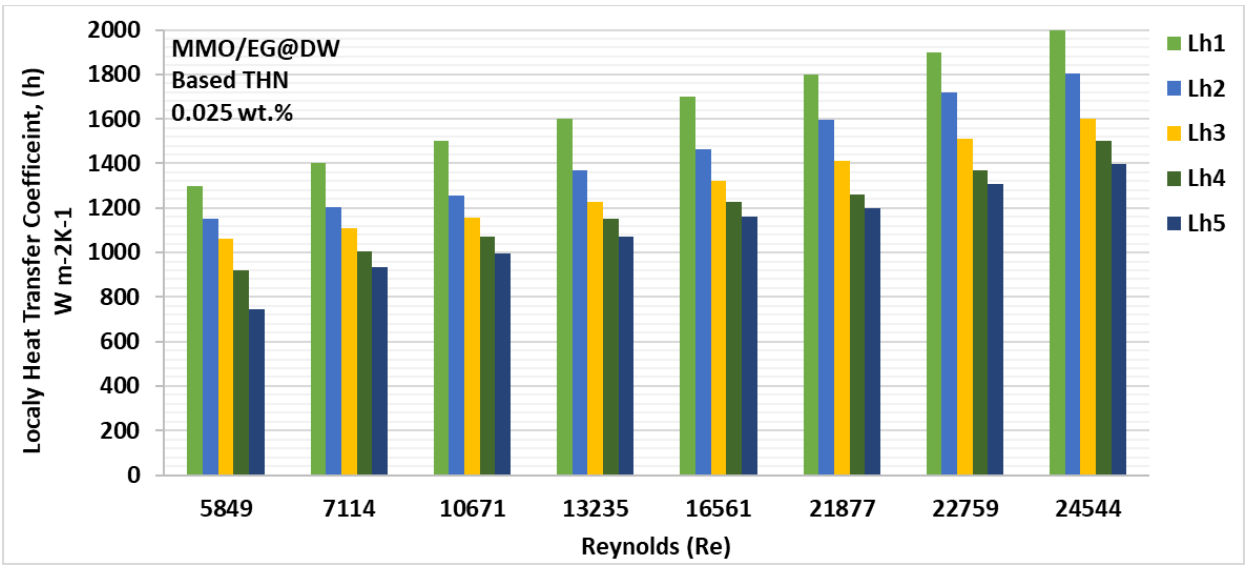


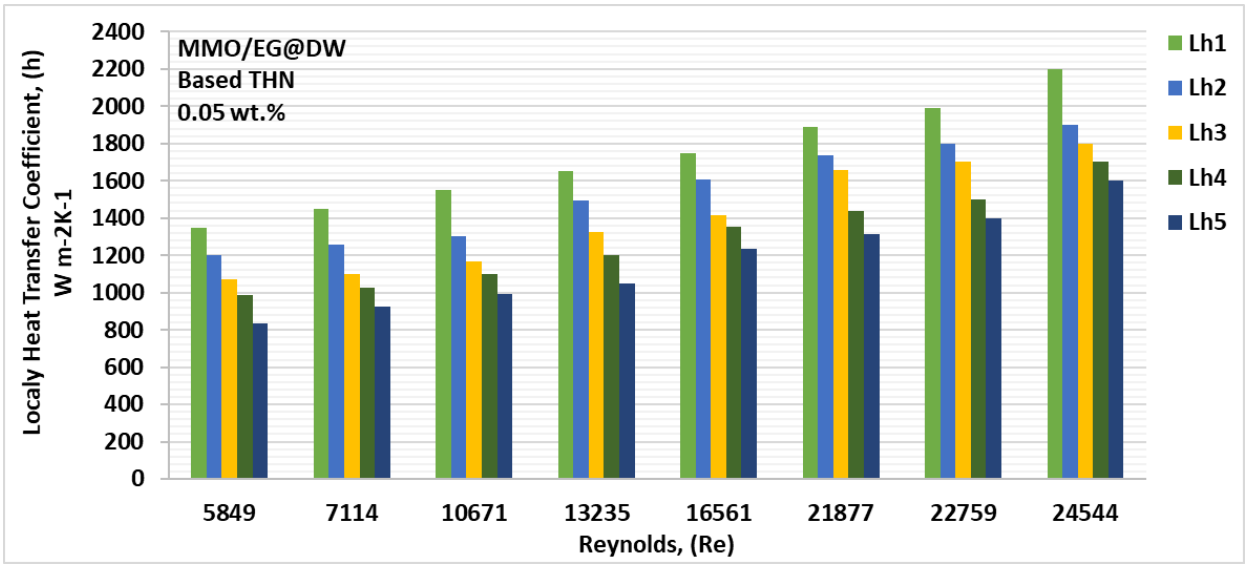
Fig.7 **a)** CHTC analysis of EG@DW and Ternary Hybrid Nanofluids (THN), **b)** Nusselt (Nu) number measurements and **c)** Comparison among experimental and model data.

5.1. Local Heat Transfer Coefficient, LHTC and Local Nusselt Number (LNu) Measurements of MMO/EG@DW based THN in Pipe Heat Exchanger

The heat transfer test section is made of stainless steel, 1.2m long, with 0.1cm of its thickness insulated with a heating wire and glass wool to protect from heat losses, as shown in Fig.2. The

total 1-meter length of the test section was considered an active region where the constant heat flux of 10092.41 W^2/K was applied. Five K-type thermocouples were placed over the surface of the test section and calibrated carefully. Further, all the K-Type thermocouples were connected to a digital data logger. The current study was also focused on the measurement of CHTC values at varying points of the test section, which are known as local convective heat transfer (LCHTC). The measurements of local convective heat transfer were carried out at room temperature, and a total of 8 flow rates were considered. A total of 40 experimental runs were performed for all EG@DW base fluids and all wt.% concentrations of the MMO/EG@DW based THN. All Fig.8a-d are evidence of CHTC improvement for varying fluids and nanofluids, where all the wt.% concentrations of 0.025 wt.%, 0.05 wt.%, 0.075 wt.% and 0.1 wt.% of MMO/EG@DW based THN showed significant enhancements in CHTC locally at varying points against all the flow rates. The pure EG@DW base fluid showed a lesser improvement in LCHTC as compared to the nanofluids. At 0.025 wt.%, the enhancement in LCHTC was about 2000 W/m. K. At 0.05 wt.%, the improvement was recorded at about 2210 W/m. K. At 0.075 wt.%, the increment was observed at about 2310 W/m.K, and then finally a great enhancement in LCHTC was attained at the higher 0.1 wt.% concentration, about 3120 W/m.K. This enhancement is significantly attributable to the use of mixed metal oxides MMO together at the same ratio %.


MMO/EG@DW
Based THN
0.025 wt.%
Localy Heat Transfer Coefficeint, (h)
W m-2K-1
2000
1800
1600
1400
1200
1000
800
600
400
200
0
5849
7114
10671
13235
16561
21877
22759
24544
Reynolds (Re)
Lh1
Lh2
Lh3
Lh4
Lh5


MMO/EG@DW
Based THN
0.05 wt.%
Localy Heat Transfer Coefficient, (h)
W m-2K-1
2400
2200
2000
1800
1600
1400
1200
1000
800
600
400
200
0
5849
7114
10671
13235
16561
21877
22759
24544
Reynolds, (Re)
Lh1
Lh2
Lh3
Lh4
Lh5

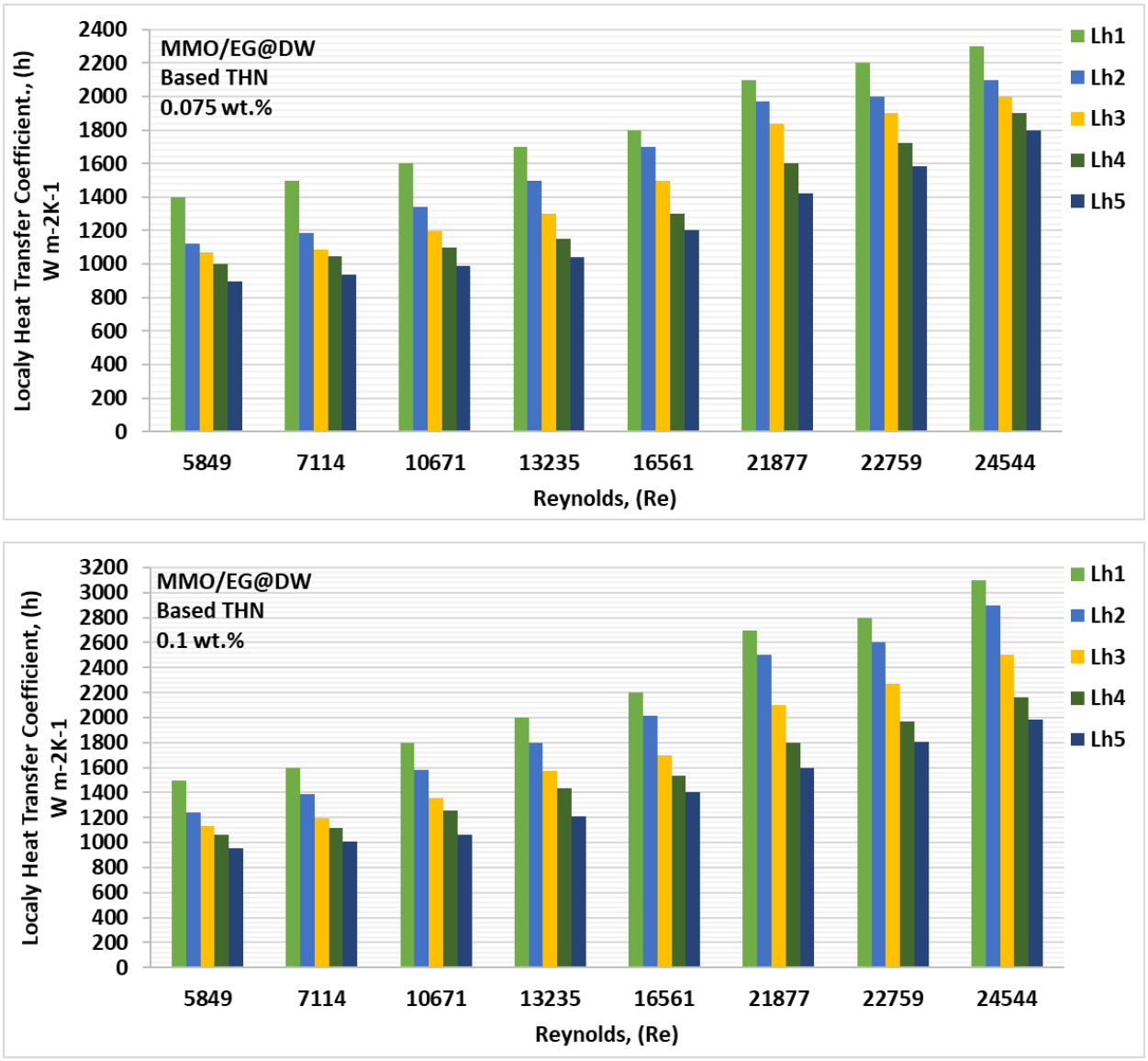
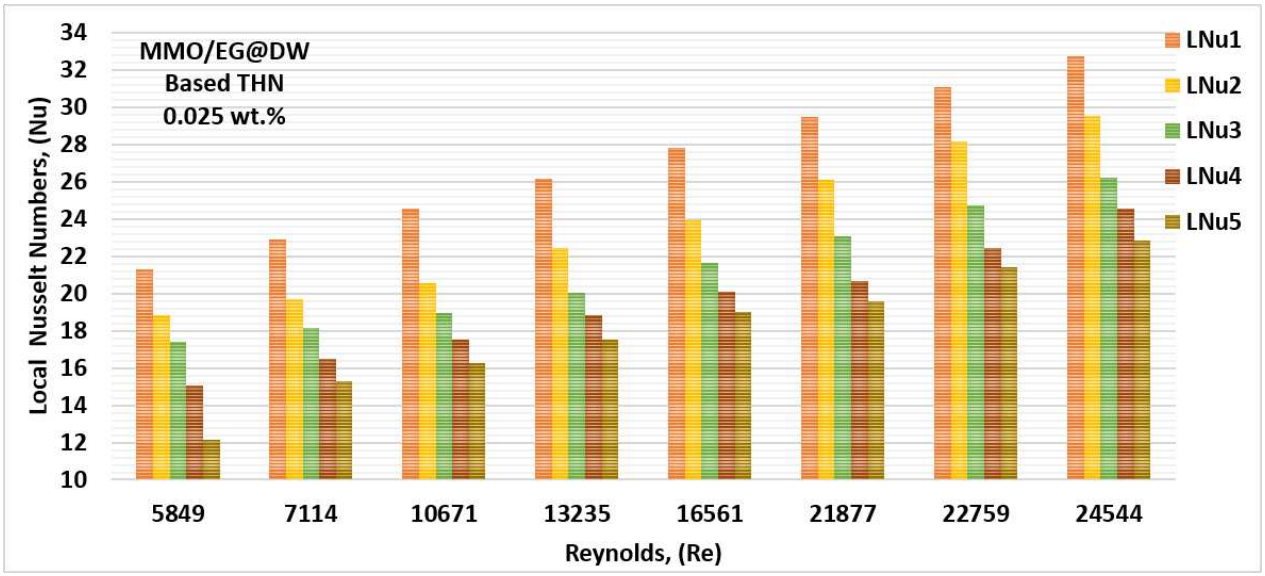
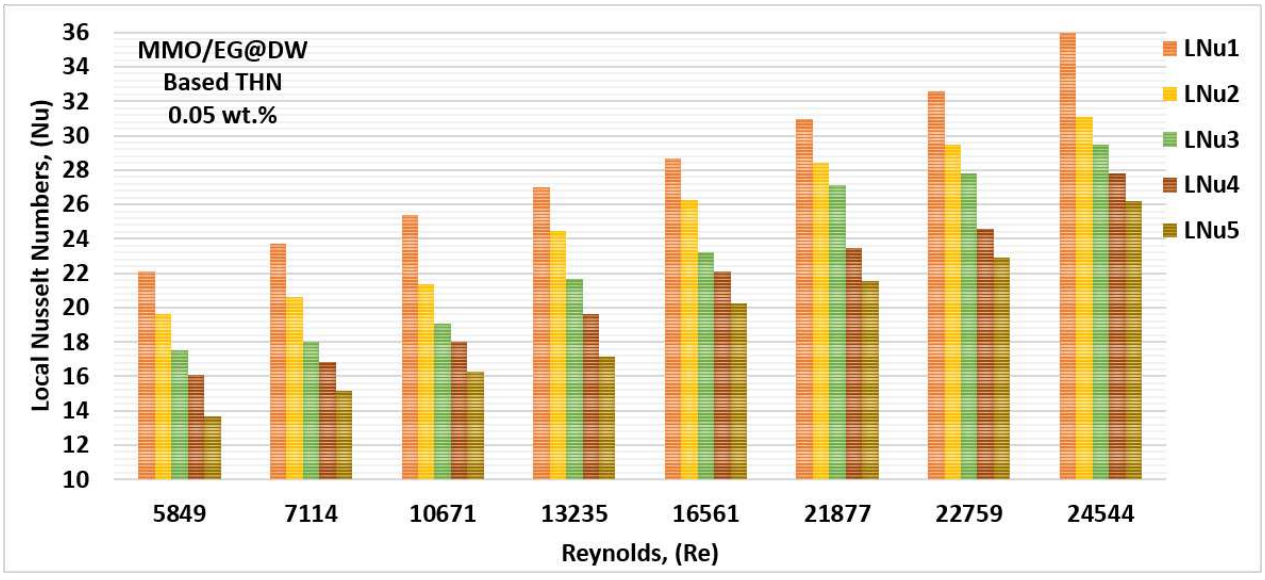


Fig.8a-d Local CHTC of Ternary Hybrid Nanofluids (THN) at varying wt.% concentrations.

Based on all the above conditions considered for the measurement of LCHTC, the local Nusselt numbers (Nu) were calculated for all the EG@DW and varying 0.025 wt.%, 0.05 wt.%, 0.075 wt.% and 0.1 wt.% concentrations of the MMO/EG@DW based THN locally at varying points of the test section shown in Fig.9a-d. The same active area (1m) of the test section was taken for the Nusselt analysis. Like the local heat transfer of the EG@DW base fluid, a lower Nusselt (Nu) increase was attained, which is due to the absence of MMO in the base fluid. The greater enlargement of Nusselt (Nu) numbers was obtained at 0.1 wt.% of the MMO/EG@DW based

THN, which is about 55; at 0.075 wt.% concentration, the improvement was about 39; at 0.05 wt.% concentration, the improvement was about 38; and finally, the lesser improvement in local Nusselt (Nu) number was about 34. This enhancement in all wt.% concentrations is mainly due to the maximum existence of the mixed metal oxide MMO in the mixture of EG@DW base fluid.





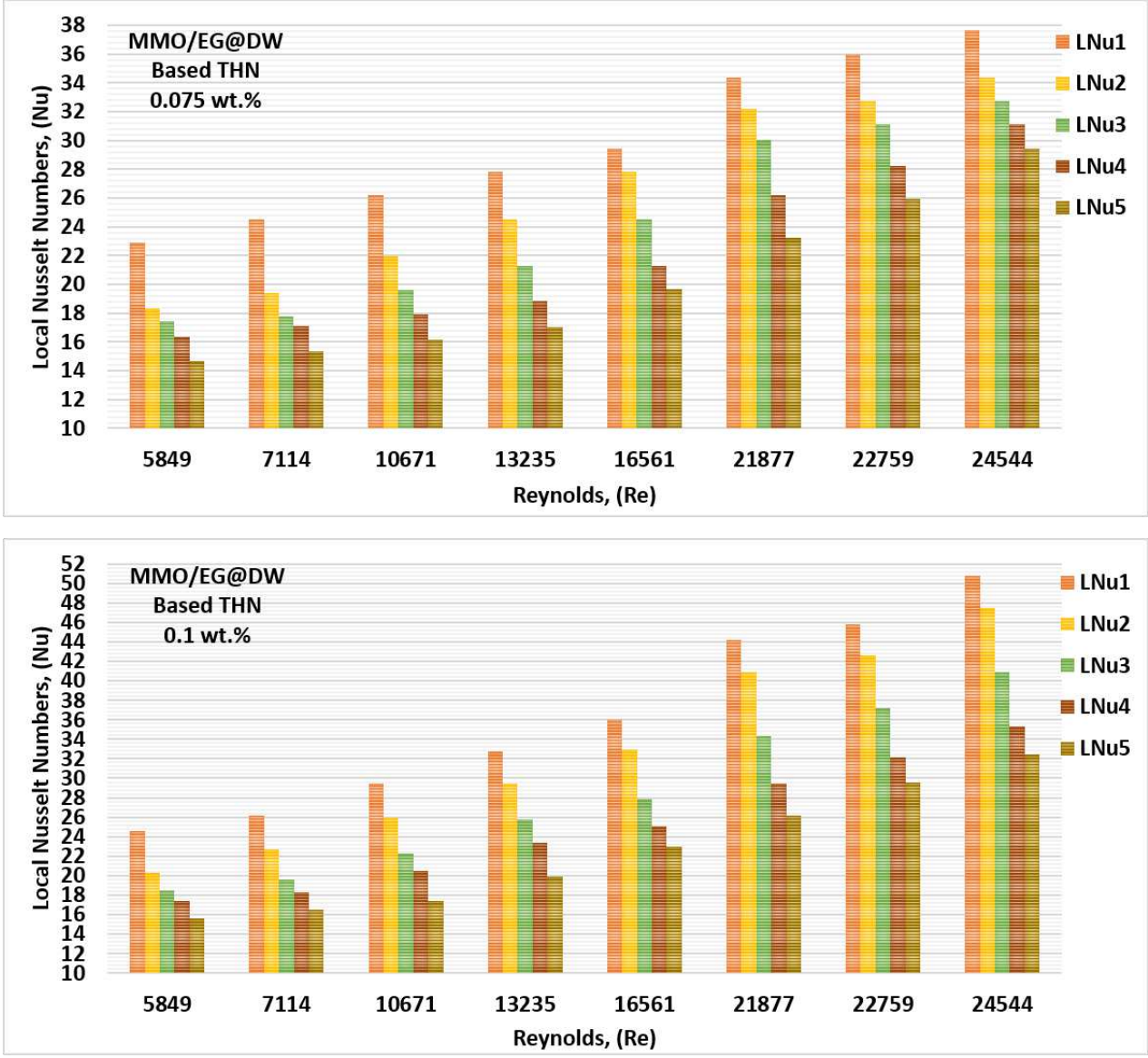


Fig.9a-d Local Nusselt (Nu) numbers of Ternary Hybrid Nanofluids (THN) at varying wt.% concentrations.

5.2. Hydrodynamic Characteristics of MMO/EG@DW based THN and EG@DW base fluid.

The pressure loss affects the overall performance of any thermal system where heat management is the utmost requirement to keep the system running. Various conventional cooling liquids have been used for thermal management in the past, where pressure loss control was given priority. The pressure loss of MMO/EG@DW based THN running in a closed heat exchanger of circular geometry was inspected against different Reynolds (Re) numbers, and key outcomes are reported

here in Fig. 10a. Eq.12 was deployed to measure the associated friction loss values, and results are also presented here in Fig.10b against the varying Reynold (Re) numbers. The key change of a minor increase in pressure loss and friction loss, recorded at all wt.% concentrations of MMO/EG@DW based nanofluids and Reynolds numbers, which is a little bit higher than that of an EG@DW base fluid. The EG@DW base fluid and all the 0.025 wt.%, 0.05 wt.%, 0.075 wt.%, and 0.1 wt.% concentrations of MMO/EG@DW based THN showed a linear increase in pressure drop across the heat exchanger at all the flow rates (Reynolds numbers). The lowest pressure drop was recorded for the EG@DW base fluid, which is not due to the presence of MMO, while a higher pressure drop was recorded at a maximum of 0.1 wt.% at the higher Reynolds number of 24544. Similarly, all other wt.% of MMO/EG@DW based THN showed a slight increase in pressure loss, which is due to their viscosity and density.

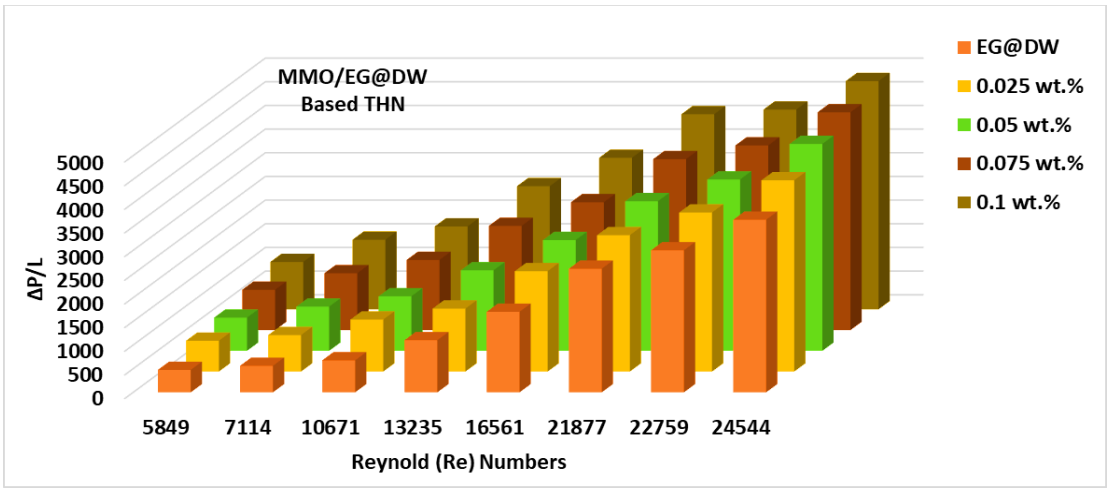
Further, the friction behaviour was observed against both Reynold (Re) numbers and wt.% concentrations as given in Fig.10b. A higher increase in friction factor was observed of~ 0.055, 0.042, 0.04, 0.035 at all 0.025 wt.%, 0.05 wt.%, 0.075 wt.% and 0.1 wt.% concentrations of MMO/EG@DW based THN individually and the lowest friction of~ 0.03 was noticed for pure EG@DW base fluid. All these increments in friction were recorded at the lower Reynold (Re) number of 5849. As the Reynolds numbers started increasing, the friction decreased for all the fluids and THN. The lower friction was noticed at the higher Reynold (Re) numbers of 24544 at all the wt.% concentrations. The rise in friction is chiefly attributed to the viscosity values of both the base fluid and THN. In addition, the nanofluid velocity plays a great role in raising the pressure loss and friction as compared with the EG@DW base fluid for the forced CHTC systems. This problem could be addressed by reviewing Eq.12 for both pressure loss and friction. Fig.10c represents the behaviours of the velocity changes corresponding to all the chosen flow rates and

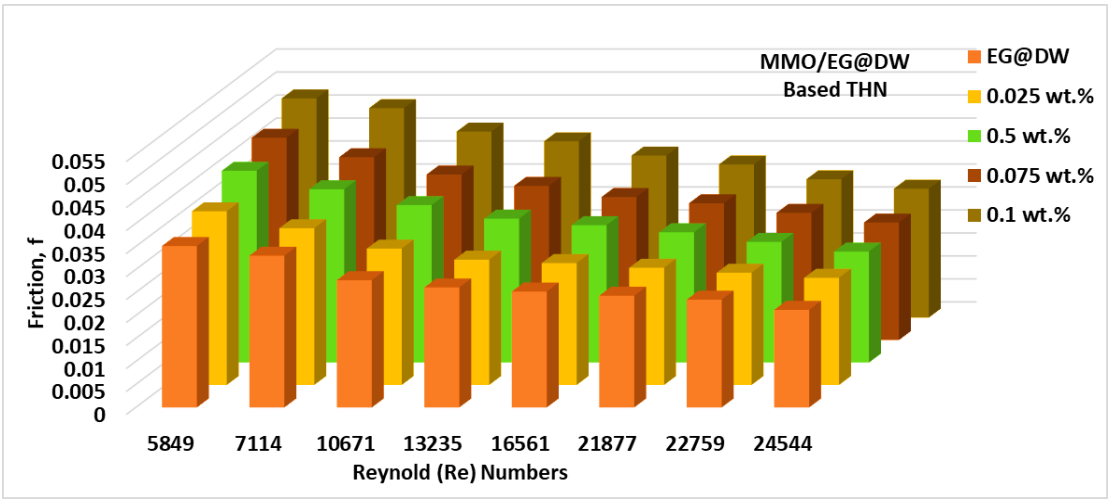
the relative pumping power that is needed to pump the EG@DW base fluid or THN in the heat exchanger, and affects the performance of the thermal system. To overcome energy loss and save energy usage, power consumption and its associated characteristics are very important in any heat transfer setup. The relative pumping power of all EG@DW base fluids and MMO/EG@DW based THN is governed by Eq.13, and the key outcomes are stated in Fig.10d at varying wt.% concentrations. A very minor increase in pumping power was recorded at a higher 0.1 wt.% concentration of the MMO/EG@DW based THN, which happened due to the lesser addition of MMO in the metal oxide together. The present study uses the use of mixed metal oxides MMO as a THN that can be used in heating and cooling devices, namely heat exchangers, solar collectors, boilers, cooling towers, engine cooling, or drill bit cooling, etc., to assess their economic performance.

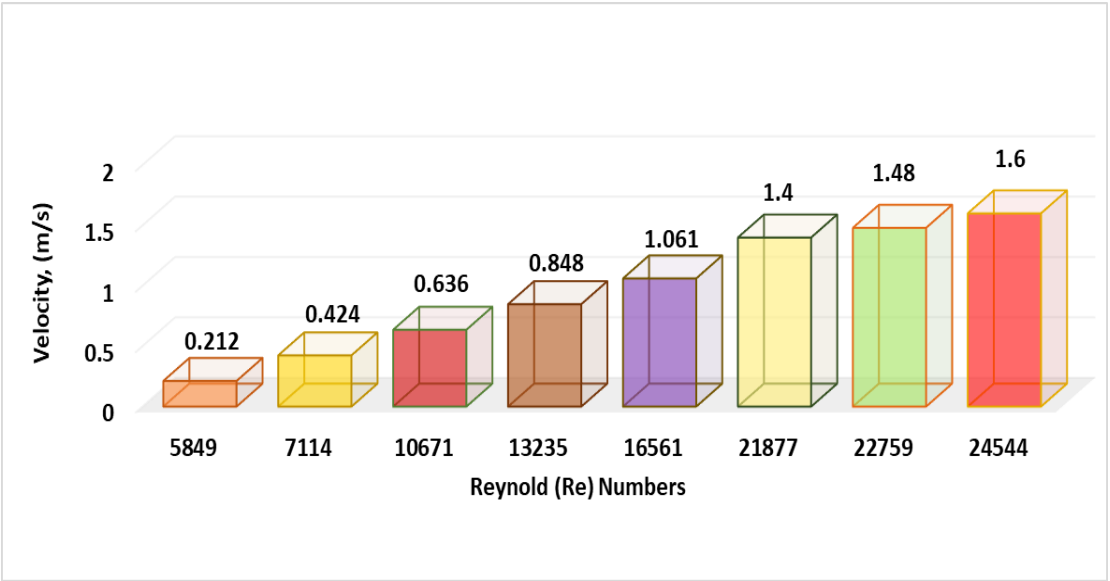
The economic performance of a heat transfer nanofluid is quantified by its performance index, defined as the ratio of the nanofluid's heat transfer increase to its pressure drop penalty, both relative to the base fluid. This index captures the trade-off between thermal benefit and hydraulic penalties caused by nanoparticles. Using the following Equ 16 or Equ 17, we evaluated the performance index for all the wt.% concentrations of MMO/EG@DW based THN. Fig.10e shows the overall performance of all varying wt.% concentrations, where it can be clearly seen that the change in concentration and flow rate impacts the performance of nanofluids. The performance of all wt.% is greater than that, which indicates the advantage of using MMO/EG@DW based THN nanofluids in thermal management systems.

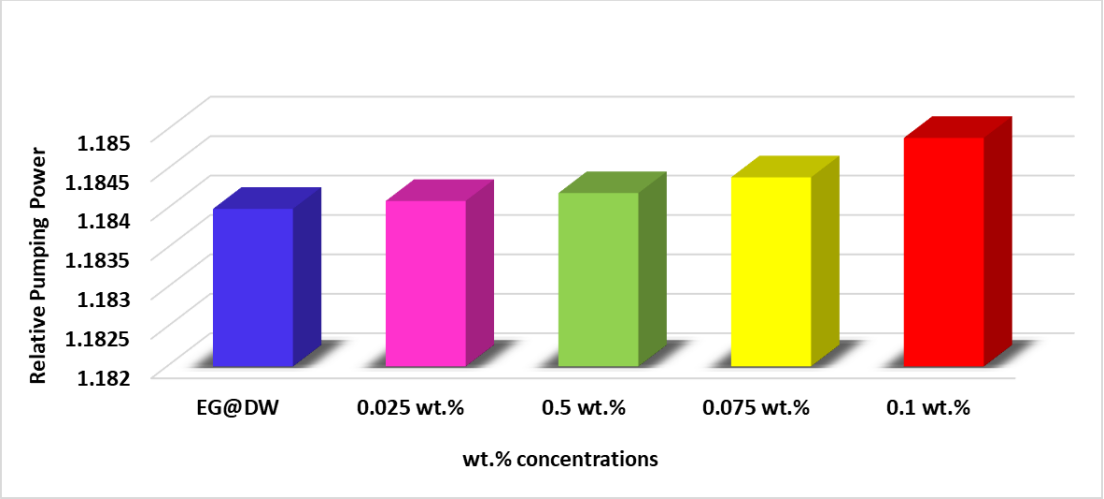
$$Performance\ Index = \frac{h_{nf}/h_{bf}}{(\frac{\Delta P}{L})_{nf}/(\frac{\Delta P}{L})_{bf}} \quad 16$$

$$\epsilon = \frac{h_{nf}/h_{bf}}{\Delta P_{nf}/\Delta P_{bf}} = \frac{R_h}{R_{\Delta h}} \quad 17$$


MMO/EG@DW
Based THN
EG@DW
0.025 wt.%
0.05 wt.%
0.075 wt.%
0.1 wt.%
ΔP/L
5000
4500
4000
3500
3000
2500
2000
1500
1000
500
0
5849
7114
10671
13235
16561
21877
22759
24544
Reynold (Re) Numbers


MMO/EG@DW
Based THN
EG@DW
0.025 wt.%
0.5 wt.%
0.075 wt.%
0.1 wt.%
Friction, f
0.055
0.05
0.045
0.04
0.035
0.03
0.025
0.02
0.015
0.01
0.005
0
5849
7114
10671
13235
16561
21877
22759
24544
Reynold (Re) Numbers


Velocity, (m/s)
2
1.5
1
0.5
0
0.212
0.424
0.636
0.848
1.061
1.4
1.48
1.6
5849
7114
10671
13235
16561
21877
22759
24544
Reynold (Re) Numbers



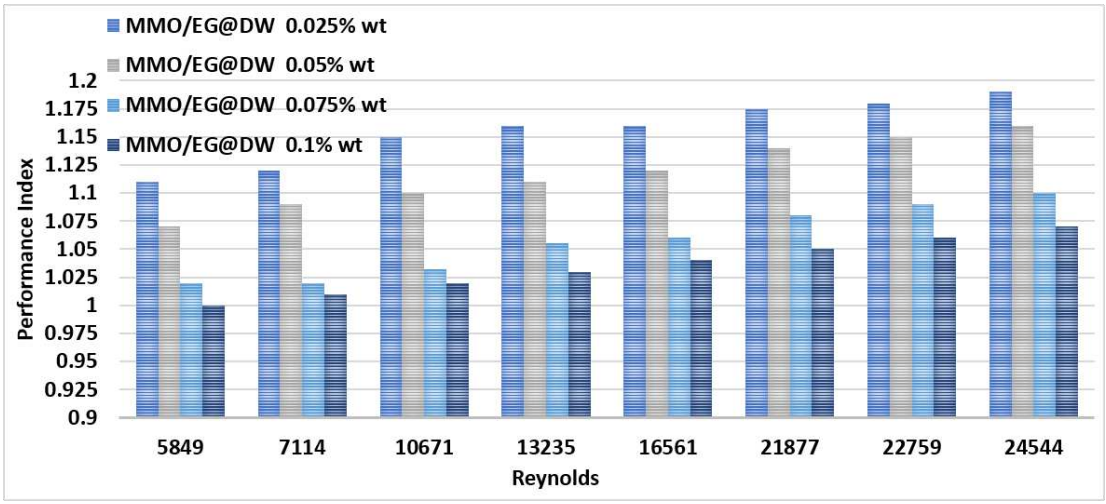


Fig.8a-e **a)** Pressure loss of Ternary Hybrid Nanofluids (THN) at varying wt.% concentrations, **b)** Friction coefficient, **c)** Velocity changes and **d)** Relative pumping power, and e) Hydrothermal performance index profile of all nanofluids.

1. CONCLUSION

Different metal oxide based hybrid/composite preparation methods were established effectively to prepare well stable and highly dispersed MMO/DW based THN nanofluids, using them as a nano coolant to improve the CHT characteristics and thermophysical and hydrodynamic characteristics of a straight stainless steel based heat exchanger with circular geometry. Based on all experiments, the following key outcomes have been identified.

- The effective mixed metal oxide (MMO) based ternary hybrid nanofluids (THN) were prepared using the 2-Step Sonochemical technique and were confirmed using their homogeneous dispersion and mixing by FESEM, UV-vis and UV-vis absorbance characterizations.
- The uniform solubility and longer stability of the MMO/EG@DW based THN in a mixture of EG@DW were tested using the photographic sedimentation method, where up to 7 weeks of stability were achieved after the day of preparation.
- All the thermophysical characteristics of MMO/EG@DW based THN were observed to be well improved as compared to those offered by the pure EG@DW base fluid, indicating that the idea of mixing three different metal oxide based THN are the participating individually or collectively for their thermal and CHT improvements. The highest thermal conductivity is enhanced by up to 27% compared to the base fluid at a concentration of 0.1 wt.% and a maximum temperature of 45 °C.
- Many studies have failed to show the enhancement in all thermophysical characteristics of single nanofluids; the current study showed that mixing different metal oxides will help to improve most of the thermophysical characteristics of the nanofluids.
- The precision of the stainless steel based heat exchanger of circular geometry was validated by executing different experiments using DW as the reference fluid. The outcomes showed an excellent agreement between data coming from empirical correlations and experimental data, which are reported in the same author's other paper.
- The outcomes showed that using different metal oxides together not only helped to improve thermophysical characteristics but also resulted in a significant enhancement in CHTC of 3120 W.m/K, which was achieved at the higher wt.% and a maximum Reynolds number

of 25544 (Re), which is greater than the CHTC achieved by a pure EG@DW mixture. There was a slight increase in friction recorded up to 3.42%, which was due to the striking of nanoparticles with the walls of the heat exchanger. These outcomes were obtained within turbulent flow at a constant heat flux of 10092.41 W/m^2.

- The outcomes were greatly promising because of the pumping power, which was recorded very near the EG@DW base fluid. Overall, the use of mixed metal oxides based THN showed greater enhancement in both thermophysical and heat transfer characteristics with low pumping power penalty.

ACKNOWLEDGEMENT

The author would like to extend great thanks to the State Key Laboratory of Photovoltaic Science and Technology, College of Future Information Technology, Fudan University, Shanghai 200438, China, for providing me with all the possible opportunities to lead my research successfully.

Funding Declaration:

The author did not receive financial support or funding from any organization for the submitted work.

DATA AVAILABILITY STATEMENT

The University of Malaya and Fudan University have a policy requiring the preservation and protection of research documents, data, and related materials. Under exceptional circumstances, the University management may grant special permission for the temporary release of specific sections of data, subject to a nondisclosure agreement (NDA). In view of this policy, we respectfully request the disclosure of raw data.

REFERENCES

1. Wang, X., et al., Nanofluids application in machining: a comprehensive review. The International Journal of Advanced Manufacturing Technology, 2023.
2. Yasmin, H., et al. Thermal Conductivity Enhancement of Metal Oxide Nanofluids: A Critical Review. Nanomaterials, 2023. 13, DOI: 10.3390/nano13030597.

3. Giwa, S.O., et al., A review of magnetic field influence on natural convection heat transfer performance of nanofluids in square cavities. Journal of Thermal Analysis and Calorimetry, 2021. 145(5): p. 2581-2623.
4. Giwa, S.O., et al., Magnetohydrodynamic convection behaviours of nanofluids in non-square enclosures: A comprehensive review. Mathematical Methods in the Applied Sciences, 2020. n/a(n/a).
5. Ambreen, T. and M.-H. Kim, Heat transfer and pressure drop correlations of nanofluids: A state of art review. Renewable and Sustainable Energy Reviews, 2018. 91: p. 564-583.
6. Murshed, S.M.S., et al. Experimental Research and Development on the Natural Convection of Suspensions of Nanoparticles—A Comprehensive Review. Nanomaterials, 2020. 10, DOI: 10.3390/nano10091855.
7. Adnan, et al., Nanoparticles diameter based thermal conductivity aspects for thermal application in nanofluid flow through Riga device associated to solar radiations and convective heating. ZAMM - Journal of Applied Mathematics and Mechanics / Zeitschrift für Angewandte Mathematik und Mechanik, 2025. 105(10): p. e70240.
8. Khan, Y., et al., Impact of chemical reaction on thermal magnetized hybrid nanofluid over a curved stretching surface. Results in Engineering, 2025. 27: p. 105556.
9. Adnan, et al., Challenging thermal mechanisms in nanofluid wedge flow over a melting surface: applications of Al2O3 and CuO nanomaterials. Multidiscipline Modeling in Materials and Structures, 2025. 21(6): p. 1513-1528.
10. Bani-Fwaz, M.Z., et al., Significance of Fe3O4/MnZnFe2O4 nanoparticles for thermal efficiency of ethylene glycol: Analysis for single-phase nanofluid flow using Cattaneo Christov theory. Modern Physics Letters B, 2025. 39(24): p. 2550105.
11. Adnan, et al., Non-Linear thermal radiations impacts on entropy and heat transfer mechanisms in tetra Nanofluid: Investigation for Sakiadis model. Journal of Radiation Research and Applied Sciences, 2025. 18(3): p. 101750.
12. Iqbal, M., et al., Critical analysis of thermal conductivity enhancement of alumina–water nanofluids. Journal of Thermal Analysis and Calorimetry, 2023.
13. Ahmed, W., et al., Effects of thermophysical, hydrodynamics and thermal characteristics of well stable metallic nanofluids on energy transportation. Journal of Thermal Analysis and Calorimetry, 2022. 147(23): p. 13879-13900.
14. Sajid, M.U., et al., Spectrum splitting through CuS–ZnO/water hybrid nanofluid for agricultural greenhouse cooling applications: An experimental study. Journal of Thermal Analysis and Calorimetry, 2023. 148(16): p. 8387-8401.
15. Raki, E., M. Afrand, and A. Abdollahi, Influence of magnetic field on boiling heat transfer coefficient of a magnetic nanofluid consisting of cobalt oxide and deionized water in nucleate regime: An experimental study. International Journal of Heat and Mass Transfer, 2021. 165: p. 120669.
16. Abdollahi, A., et al., Experimental Study of Pool Boiling Heat Transfer Coefficient for DI-Water-Based Nanofluids Containing Nickel Oxide in a Constant Magnetic Field. International Journal of Thermophysics, 2023. 44(4): p. 62.
17. Xiaohong, D., et al., Statistical estimation the thermal conductivity of MWCNTs-SiO2/Water-EG nanofluid using the ridge regression method. Physica A: Statistical Mechanics and its Applications, 2020. 537: p. 122782.
18. Almitani, K.H., et al., Effects of surfactant on thermal conductivity of aqueous silica nanofluids. Journal of Molecular Liquids, 2021. 327: p. 114883.

19. Ahmed, W., et al., One-pot sonochemical synthesis route for the synthesis of ZnO@TiO2/DW hybrid/composite nanofluid for enhancement of heat transfer in a square heat exchanger. Journal of Thermal Analysis and Calorimetry, 2021. 143(2): p. 1139-1155.
20. Kiradjiev, K.B., et al., Maxwell-type models for the effective thermal conductivity of a porous material with radiative transfer in the voids. International Journal of Thermal Sciences, 2019. 145: p. 106009.
21. Ma, B., et al. Estimation of Measurement Uncertainties for Thermal Conductivity of Nanofluids using Transient Plane Source (TPS) Technique. in 2018 17th IEEE Intersociety Conference on Thermal and Thermomechanical Phenomena in Electronic Systems (ITherm). 2018.
22. Petukhov, B., Heat transfer and friction in turbulent pipe flow with variable physical properties. Advances in heat transfer, 1970. 6(503): p. i565.
23. Gnielinski, V., New equations for heat and mass transfer in the turbulent flow in pipes and channels. NASA STI/recon technical report A, 1975. 75: p. 8-16.
24. Petukhov, B.S., Heat Transfer and Friction in Turbulent Pipe Flow with Variable Physical Properties, in Advances in Heat Transfer, J.P. Hartnett and T.F. Irvine, Editors. 1970, Elsevier. p. 503-564.
25. Blasius, H. Grenzschichten in Flüssigkeiten mit kleiner Reibung.
26. Mansour, R.B., N. Galanis, and C.T. Nguyen, Effect of uncertainties in physical properties on forced convection heat transfer with nanofluids. Applied Thermal Engineering, 2007. 27(1): p. 240-249.
27. Sarsam, W.S., et al., Stability and thermophysical properties of non-covalently functionalized graphene nanoplatelets nanofluids. Energy Conversion and Management, 2016. 116: p. 101-111.
28. Nabati Shoghl, S., J. Jamali, and M. Keshavarz Moraveji, Electrical conductivity, viscosity, and density of different nanofluids: An experimental study. Experimental Thermal and Fluid Science, 2016. 74: p. 339-346.
29. Li, X., D. Zhu, and X. Wang, Evaluation on dispersion behavior of the aqueous copper nano-suspensions. Journal of Colloid and Interface Science, 2007. 310(2): p. 456-463.
30. Sepehrnia, M., et al., Examining rheological behavior of CeO2-GO-SA/10W40 ternary hybrid nanofluid based on experiments and COMBI/ANN/RSM modeling. Scientific Reports, 2022. 12(1): p. 22054.
31. Huminic, G. and A. Huminic, Entropy generation of nanofluid and hybrid nanofluid flow in thermal systems: A review. Journal of Molecular Liquids, 2020. 302: p. 112533.
32. Said, Z., et al., Synthesis, stability, density, viscosity of ethylene glycol-based ternary hybrid nanofluids: Experimental investigations and model -prediction using modern machine learning techniques. Powder Technology, 2022. 400: p. 117190.
33. Said, Z., et al., Optimizing density, dynamic viscosity, thermal conductivity and specific heat of a hybrid nanofluid obtained experimentally via ANFIS-based model and modern optimization. Journal of Molecular Liquids, 2021. 321: p. 114287.
34. Kumar, N. and S.S. Sonawane, Experimental study of thermal conductivity and convective heat transfer enhancement using CuO and TiO2 nanoparticles. International Communications in Heat and Mass Transfer, 2016. 76: p. 98-107.
35. Vakili, M., et al., Experimental investigation and modeling of thermal conductivity of CuO–water/EG nanofluid by FFBP-ANN and multiple regressions. Journal of Thermal Analysis and Calorimetry, 2017. 129(2): p. 629-637.

36. Singh, R.K., et al., Experimental investigation of thermal conductivity and specific heat of nanoparticles mixed cutting fluids. Materials Today: Proceedings, 2017. 4(8): p. 8587-8596.
37. Aberoumand, S. and A. Jafarimoghaddam, Experimental study on synthesis, stability, thermal conductivity and viscosity of Cu–engine oil nanofluid. Journal of the Taiwan Institute of Chemical Engineers, 2017. 71: p. 315-322.
38. Ahmadi, M.H., et al., A review of thermal conductivity of various nanofluids. Journal of Molecular Liquids, 2018. 265: p. 181-188.
39. Teng, T.-P., et al., The effect of alumina/water nanofluid particle size on thermal conductivity. Applied Thermal Engineering, 2010. 30(14): p. 2213-2218.
40. Sharifpur, M., et al., Experimental investigation and model development for thermal conductivity of α-Al2O3-glycerol nanofluids. International Communications in Heat and Mass Transfer, 2017. 85: p. 12-22.
41. Alawi, O.A., et al., Thermal conductivity and viscosity models of metallic oxides nanofluids. International Journal of Heat and Mass Transfer, 2018. 116: p. 1314-1325.
42. Ahmed, W., et al., Experimental investigation of convective heat transfer growth on ZnO@TiO2/DW binary composites/hybrid nanofluids in a circular heat exchanger. Journal of Thermal Analysis and Calorimetry, 2021. 143(2): p. 879-898.
43. Ahmed, W., et al., Effect of ZnO-water based nanofluids from sonochemical synthesis method on heat transfer in a circular flow passage. International Communications in Heat and Mass Transfer, 2020. 114: p. 104591.
44. Tsai, C.Y., et al., Effect of structural character of gold nanoparticles in nanofluid on heat pipe thermal performance. Materials Letters, 2004. 58(9): p. 1461-1465.
45. Chavan, D. and A.T. Pise, Experimental investigation of convective heat transfer agumentation using Al2O3/water nanofluid in circular pipe. Heat and Mass Transfer, 2015. 51(9): p. 1237-1246.
46. Akram, N., et al., A facile, green fabrication of aqueous nanofluids containing hydrophilic functionalized carbon nanotubes toward improving heat transfer in a closed horizontal flow passage. Powder Technology, 2022. 404: p. 117451.
47. Ahmed, W., et al. Evaluation on Enhanced Heat Transfer Using Sonochemically Synthesized Stable Zno-Eg@Dw Nanofluids in Horizontal Calibrated Circular Flow Passage. Energies, 2021. 14, DOI: 10.3390/en14092400.
48. Gnielinski, V., New equations for heat and mass transfer in the turbulent flow in pipes and channels. NASA STI/recon technical report A, 1975. 41(1): p. 8-16.
49. Duangthongsuk, W. and S. Wongwises, Effect of thermophysical properties models on the predicting of the convective heat transfer coefficient for low concentration nanofluid. International Communications in Heat and Mass Transfer, 2008. 35(10): p. 1320-1326.